Radiology of Osteoporosis

6

Michael Jergas

CONTENTS

Michael Jergas, MD
Priv.-Doz., Department of Radiology and Nuclear Medicine, St. Elisabeth-Krankenhaus, Werthmannstrasse 1, 50935 Cologne, Germany

The term osteoporosis is widely used clinically to mean generalized loss of bone, or osteopenia, accompanied by relatively atraumatic fractures of the spine, wrist, hips or ribs. Because of uncertainties of specific radiologic interpretation, the term osteopenia ("poverty of bone") has been used as a generic designation for radiographic signs of decreased bone density. Radiographic findings suggestive of osteopenia and osteoporosis are frequently encountered in everyday medical practice and can result from a wide spectrum of diseases ranging from highly prevalent causes such as postmenopausal and involutional osteoporosis to rare endocrinologic and hereditary or acquired disorders (Table 6.1). Histologically, in each of these disorders there is a deficient amount of osseous tissue, although different pathogenic mechanisms may be involved. Conventional radiography is widely available, and alone, or in conjunction with other imaging techniques it is widely used for the detection of complications of osteopenia, for the differential diagnosis of osteopenia, or for follow-up examinations in specific clinical settings. Bone scintigraphy, computed tomography and magnetic resonance imaging are additional diagnostic methods that are applied almost routinely to aid in the differential diagnosis of osteoporosis and its sequelae.

6.1 Radiographic Findings in Osteopenia and Osteoporosis

Knowledge of both the physical nature of X-ray absorption by biologic tissues as well as the histopathologic changes leading to osteopenia and osteoporosis is required to understand the radiographic findings. The absorption of X-rays by a tissue depends on the quality of the X-ray beam, the character of the atoms composing the tissue, the physical density

Table 6.1. Disorders associated with radiographic osteoporosis (osteopenia).

I. Primary osteoporosis
1. Involutional osteoporosis (postmenopausal and senile)
2. Juvenile osteoporosis
II. Secondary osteoporosis
A. Endocrine
1. Adrenal cortex (Cushing's disease)
2. Gonadal disorders (hypogonadism)
3. Pituitary (hypopituitarism)
4. Pancreas (diabetes)
5. Thyroid (hyperthyroidism)
6. Parathyroid (hyperparathyroidism)
B. Marrow replacement and expansion
1. Myeloma
2. Leukemia
3. Metastatic disease
4. Gaucher's disease
5. Anemias (sickle cell disease, thalassemia)
C. Drugs and substances
1. Corticosteroids
2. Heparin
3. Anticonvulsants
4. Immunosuppressants
5. Alcohol (in combination with malnutrition)
D. Chronic disease
1. Chronic renal disease
2. Hepatic insufficiency
3. Gastrointestinal malabsorption
4. Chronic inflammatory polyarthropathies
5. Chronic immobilization
E. Deficiency states
1. Vitamin D
2. Vitamin C (scurvy)
3. Calcium
4. Malnutrition
F. Inborn errors of metabolism
1. Osteogenesis imperfecta
2. Homocystinuria

of the tissue, and the thickness of the penetrated structure. The amount of X-ray absorption defines the density of X-ray shadow that a tissue casts on the film. Because absorption rises with the third power of the atomic number, and because calcium has a high atomic number, it is primarily the amount of calcium that affects the X-ray absorption of bone. The amount of calcium per unit mineralized bone volume in osteoporosis remains constant at about 35% (Albright et al. 1941; LeGeros 1994). Therefore, a decrease in the mineralized bone volume results in a decrease of the total bone calcium and consequently a decreased absorption of the X-ray beam. On the X-ray film this phenomenon is referred to as increased radiolucency.

As bone mass is lost, changes in bone structure occur, and these can be observed radiographically (Fig. 6.1). Bone is composed of two compartments, cortical bone and trabecular bone. The structural changes seen in cortical bone represent bone resorption at different sites (e.g., the inner and outer surfaces of the cortex, or within the cortex in the Haversian and Volkmann channels). These three sites (endosteal, intracortical and periosteal) may react differently to distinct metabolic stimuli, and careful investigation of the cortices may be of value in the differential diagnosis of metabolic disease affecting the skeleton.

Cortical bone remodeling typically occurs in the endosteal "envelope", and the interpretation of subtle changes in this layer may be difficult at times. With increasing age, there is a widening of the marrow canal due to an imbalance of endosteal bone formation and resorption that leads to a "trabeculization" of the inner surface of the cortex. Endosteal scalloping due to resorption of the inner bone surface can be seen in high bone turnover states such as reflex sympathetic dystrophy.

Intracortical bone resorption may cause longitudinal striation or tunneling, predominantly in the subendosteal zone. These changes are seen in various high turnover metabolic diseases affecting the bone such as hyperparathyroidism, osteomalacia, renal osteodystrophy, and acute osteoporosis from disuse or the reflex sympathetic dystrophy syndrome but also postmenopausal osteoporosis. Intracortical tunneling is a hallmark of rapid bone turnover. It is usually not apparent in disease states with relatively low bone turnover such as senile osteoporosis. Accelerated endosteal and intracortical resorption with intracortical tunneling and indistinct border of the inner cortical surface, is best depicted with high resolution radiographic techniques. Intracortical tunneling must be distinguished from nutritional foramina, which are isolated and present with an oblique orientation. Intracortical resorption is also a sign of bone viability and is not seen in necrotic or allograft bone.

Subperiosteal bone resorption is associated with an irregular definition of the outer bone surface. This finding is pronounced in diseases with a high bone turnover, principally primary and secondary

Fig. 6.1a,b. Conventional radiographs of the hand in a healthy woman (**a**) and in a patient suffering from osteoporosis (**b**). Aside from a general increase in radiolucency of the bone there is also a diminution of cortical bone and widening of the marrow space

hyperparathyroidism. However, rarely it may also be present in other diseases. Cortical thinning with expansion of the medullary cavity occurs as endosteal bone resorption exceeds periosteal bone apposition in most adults. In the late stages of osteoporosis, the cortices appear paper-thin with the endosteal surface usually being smooth.

Trabecular bone has a greater surface and responds faster to metabolic changes than does cortical (Frost 1964). These changes are most prominent in the axial skeleton and in the ends of the long and tubular bones of the appendicular skeleton (juxtaarticular), e.g., proximal femur, distal radius. These are sites with a relatively great amount of trabecular bone. Loss of trabecular bone (in cases with low rates of loss) occurs in a predictable pattern. Nonweight bearing trabeculae are resorbed first. This leads to a relative prominence of the weight bearing trabeculae. The remaining trabeculae may become thicker, which may result in a distinct radiographic trabecular pattern. For example, early changes of osteopenia in the lumbar spine typically include a rarefication of the horizontal trabeculae accompanied by a relative accentuation of the vertical trabeculae, radiographically appearing as vertical striation of the bone. With decreasing density of the trabecular bone the cortical rim of the vertebrae is accentuated, and the vertebrae may have a "picture-frame" appearance (Fig. 6.2). In addition to changes in the trabecular bone, thinning of the cortical bone occurs. Changes of the bone structure at distinct skeletal sites are assessed for the differential diagnosis of various skeletal conditions. For the evaluation of very subtle changes, such as different forms of bone resorption, high resolution radiographic techniques with optical or geometric magnification may be required (Genant et al. 1977).

The anatomic distribution of the osteopenia or osteoporosis depends on the underlying cause. Osteopenia can be generalized affecting the whole skeleton, or regional, affecting only a part of the skeleton, usually in the appendicular skeleton. Typical examples of generalized osteopenias are involutional and postmenopausal osteoporosis and osteoporosis caused by endocrine disorders such as hyperparathyroidism, hyperthyroidism, osteomalacia and hypogonadism. Regional forms of osteoporosis result from factors affecting only parts of the appendicular skeleton such as disuse, reflex sympathetic syndrome and transient osteoporosis of large

Fig. 6.2. Severe osteopenia. The transparency of the vertebral bodies matches that of the intervertebral disc space. There are multiple fractures of the vertebral endplates leading to biconcave deformities of the vertebrae as well as a severe fracture of L5

joints. The distribution of osteopenia may vary considerably between different diseases and may be suggestive of a specific diagnosis. Focal osteopenia primarily reflects the underlying cause such as inflammation, fracture or tumor.

Thus, it seems that a number of characteristic features by conventional radiography make the diagnosis of osteopenia or osteoporosis possible. However, the detection of osteopenia by conventional radiography is inaccurate since it is influenced by many technical factors such as radiographic exposure factors, film development, soft tissue thickness of the patient, etc. (Table 6.2). It has been estimated that as much as 20%–40% of bone mass must be lost before a decrease in bone density can be seen in lateral radiographs of the thoracic and lumbar spine (Lachmann and Whelan 1936). Finally, the diagnosis of osteopenia from conventional radiographs is dependent on the experience of the reader and his/her subjective interpretation (Jergas et al. 1994a).

In summary, a radiograph may reflect the amount of bone mass, histology and gross morphology of the skeletal part examined. The principal findings of osteopenia are increased radiolucency, changes in bone microstructure, e.g. rarefication of trabeculae, thinning of the cortices, eventually resulting in changes of the gross bone morphology, i.e., changes in the shape of the bone and fractures.

Table 6.2. Factors influencing the radiographic appearance of objects (Heuck and Schmidt 1960)

Radiation source
Exposure time
Film-focus distance
Anode characteristics
Voltage
Beam filtration
Object
Thickness of bone
Bone mineral content
Soft tissue composition
Scattering
Film and screen
Film granularity
Emulsion of film
Film speed
Screen properties
Film processing
Developing time
Temperature of developer
Type of developer
Type of fixer
Type of processing (automated vs. manual)

6.2 Diseases Characterized by Generalized Osteopenia

6.2.1 Involutional Osteoporosis

Involutional osteoporosis is the most common generalized skeletal disease. It has been classified as a type I or postmenopausal osteoporosis and a type II or senile osteoporosis (Albright 1947; Riggs and Melton 1983). Gallagher (1990) added a third type meaning secondary osteoporosis (Table 6.3). Even though the importance of estrogen deficiency for postmenopausal osteoporosis has been established, the distinction between the first two types of osteoporosis is not generally accepted. Distinctions between postmenopausal and senile osteoporosis may sometimes be arbitrary, and the assignment of fracture sites to the different types of osteoporosis is uncertain. Postmenopausal osteoporosis is believed to represent that process occurring in a subset of postmenopausal women, typically between the ages of 50 and 65 years. There is accelerated trabecular bone resorption related to estrogen deficiency, and the fracture pattern in this group of women primarily involves the spine and the wrist. In senile osteoporosis, there is a proportionate loss of cortical and trabecular bone. The characteristic fractures of senile osteoporosis include fractures of the hip, the proximal humerus, the tibia and the pelvis in elderly women and men, usually 75 years or older. Major factors in the etiology of senile osteoporosis include the age-related decrease in bone formation, diminished adrenal function, reduced intestinal calcium absorption and secondary hyperparathyroidism.

Table 6.3. Classification of osteoporosis acording to Albright, Riggs and Melton, and Gallagher (Table adapted from Gallagher 1992)

Type	I Postmenopausal	II Senile	III Secondary
Age	55-70	75-90	Any age
Years past menopause	5-15	25-40	-
Sex ratio (female:male)	20:1	2:1	1:1
Fracture site	Spine	Hip, spine, pelvis, humerus	Spine, hip, peripheral skeleton
Bone loss			
– Trabecular	+++	++	+++
– Cortical	+	++	+++
Contributing factor			
– Menopause	+++	++	++
– Age	+	+++	++

The radiographic appearance of the skeleton in involutional osteoporosis may include all of the aforementioned characteristics for generalized osteoporosis. The high prevalence of involutional osteoporosis with its typical radiographic manifestations has lead to numerous attempts to diagnose and quantify osteoporosis based on its radiographic characteristics.

6.2.1.1 Osteopenia and Osteoporosis of the Axial Skeleton

The radiographic manifestation of osteopenia of the axial skeleton includes increased radiolucency of the vertebrae. The vertebral body's radiographic density may assume the density of the intervertebral disk space. Further findings include vertical striation of the vertebrae due to reinforcement of vertical trabeculae in the osteopenic vertebra, framed appearance of the vertebrae ("picture framing" or "empty box") due to an accentuation of the cortical outline, and increased biconcavity of the vertebral endplates (Fig. 6.3). Biconcavity of the vertebrae results from protrusion of the intervertebral disk into the weakened vertebral body. A classification of these characteristics can be found with the Saville index (Table 6.4) (Saville 1967). This index, however, has never gained widespread acceptance, being prone to great subjectivity and experience of the reader. Doyle and colleagues (1967) found that neither of aforementioned signs of osteopenia reflect the bone mineral status of an individual reliably and cannot be used for follow-up of osteopenic patients. Thus, bone density measurements using dedicated densitometric methods have widely replaced the subjective analysis of bone density from conventional radiographs. Densitometric results may suggest osteopenia even if the bone loss is not detectable on a spine radiograph. Nevertheless, the aforementioned radiographic signs of osteoporosis have been found to be significantly related to measured bone density, and normal bone densitometry measurements may

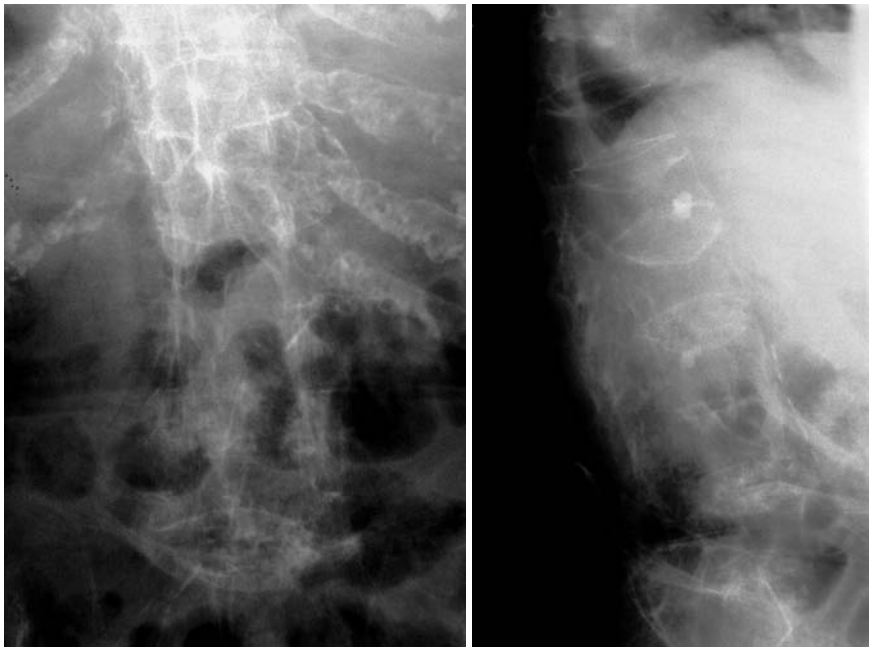

Fig. 6.3. Severe osteopenia in a patient with long-standing osteoporosis. There are multiple vertebral deformities. Due to the decreased bone density bone tissue can hardly be differentiated from soft tissue

Table 6.4. Osteopenia score for vertebrae by Saville (1967)

Grade	Radiographic appearance of vertebra
0	Normal bone density
1	Minimal loss of density; endplates begin to stand out giving a stenciled effect
2	Vertical striation is more obvious; endplates are thinner
3	More severe loss of bone density than grade 2; endplates becoming less visible
4	Ghost-like vertebral bodies; density is no greater than soft tissue; no trabecular pattern is visible

sometimes have to be considered false if the radiograph displays characteristic changes of osteopenia (Jergas et al. 1994b; Ahmed et al. 1998).

6.2.2 Vertebral Fractures and Their Diagnosis

Vertebral fractures are the hallmarks of osteoporosis, and even though one may argue that osteopenia per se may not be diagnosed reliably from spinal radiographs, spinal radiography continues to be a substantial aid in diagnosing and following vertebral fractures (Genant et al. 1993). Furthermore, along with a low bone density the vertebral fracture has been recognized as the strongest risk factor for future osteoporotic fractures (Ross et al. 1991, 1993; Kotowicz et al. 1994). Thus, the presence of vertebral fracture has become a key factor in patient evaluation as expressed in the NOF guidelines (National Osteoporosis Foundation 2000; Lenchik et al. 2004). Educational efforts, such as the Vertebral Fracture Initiative by the IOF, aim at raising the awareness of physicians to recognize the importance of vertebral fracture as a trigger for therapeutic decisions to prevent future fractures (Delmas et al. 2005).

Changes in the gross morphology of the vertebral body have a wide range of appearances from increased concavity of the end plates to a complete destruction of the vertebral anatomy in vertebral crush fractures. In clinical practice conventional radiographs of the thoracolumbar region in lateral projection are analyzed qualitatively by radiologists or experienced clinicians to identify vertebral deformities or fractures. For an experienced radiologist, this assessment generally is uncomplicated, and it can be aided by additional radiographic projections such as anteroposterior and oblique views, or by complimentary examinations such as bone scintigraphy, computed tomography (Fig. 6.4) and magnetic resonance imaging (Fig. 6.5) (McAfee et al. 1983; Ballock et al. 1992; Campbell et al. 1995; Tehranzadeh and Tao 2004).

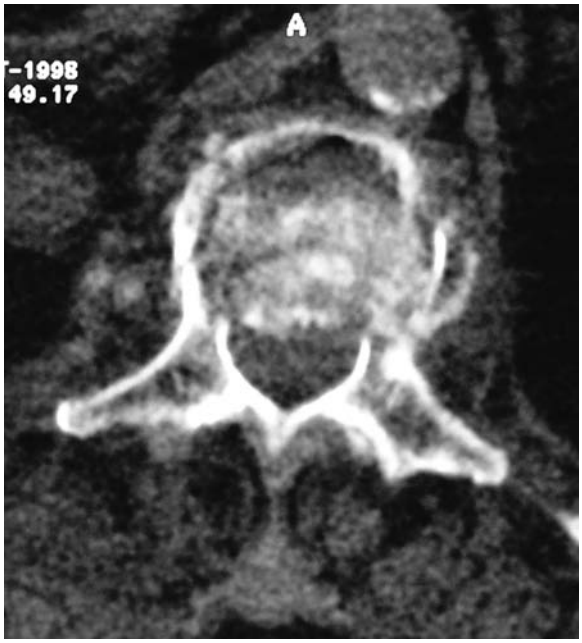

Fig. 6.4. Computed tomography of the osteoporotic fracture may reveal involvement of the posterior border as well as narrowing of the spinal canal

In the context of conducting epidemiologic studies or clinical drug trials in osteoporosis research, where vertebral fractures are an important end point, the requirements and expectations differ considerably from the clinical environment (Kleerekoper et al. 1992). The examinations are frequently performed without specific clinical indications and without specific therapeutic ramifications. The evaluation for fractures is generally limited to lateral conventional thoracolumbar radiographs, and the number of subjects to be reviewed is often quite large, requiring high efficiency. The assessment may be performed by a variety of observers with different levels of experience. The detection of vertebral fractures certainly depends on the reader's expertise. Early experience with qualitative readings indicated that considerable variability in fracture identification exists when radiologists or clinicians interpreted radiographs without specific training, standardization, reference to an atlas or prior consensus readings (Jensen et al. 1984; Deyo et al. 1985; Genant et al. 1995).

Therefore, several approaches to standardizing visual qualitative readings have been proposed and applied in clinical studies. An early approach for a standardized description of vertebral fractures was made by Smith and colleagues (1960). These authors assigned one of three grades (normal, indeterminate or osteoporotic) to a patient depending on the most severe deformity (Smith et al. 1960). The spinal radiographs were evaluated on a per patient and not on a per vertebra basis, a serious limitation for the follow-up of vertebral fractures and also for the assessment of the severity of osteoporosis. Other standardized visual approaches allow for an assess-

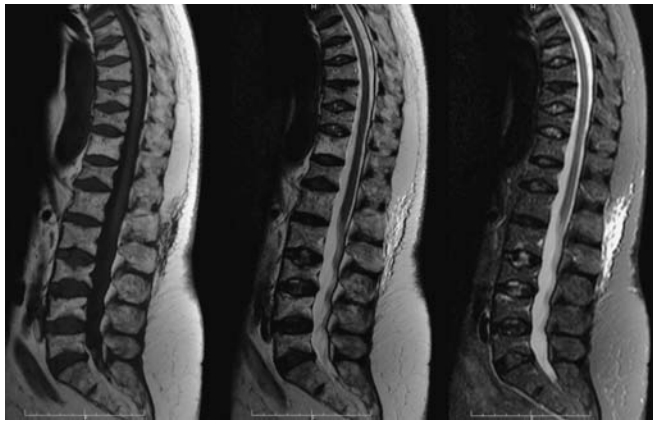

a

b

Fig. 6.5a,b. Magnetic resonance imaging of benign vertebral collapse (**a**) and metastatic disease of the spine in breast cancer (**b**). Abnormal signal that parallels the fracture, the absence of abnormal signal in non-fractured vertebrae, other vertebral deformities with normal signal and the absence of paravertebral soft tissue mass usually indicates benign vertebral collapse. Diffusion weighted images may also help differentiate between benign (low signal) and malignant (high signal) vertebral collapse

ment of vertebral deformities on a per vertebra rather than on a per patient basis and thus make a more accurate assessment of the fracture status of a person and the follow-up of individual fractures possible. Meunier et al. (1978) proposed an approach in which each vertebra is graded depending on its shape or deformity. Grade 1 is assigned to a normal vertebra without any deformity, grade 2 is assigned to a biconcave vertebra, and grade 4 is assigned to an end plate fracture or a wedged or crushed vertebra. The sum of all grades of the vertebrae T7 to L4 is the radiological vertebral index (RVI). This approach is limited since it considers only the type of the vertebral deformity, i.e., biconcavity versus fracture, without assessing fracture severity. For prevalent fractures, each fracture, whether it is diminutive or severe, would have the same weight in the RVI, and for the application of this approach to follow-up examinations this means that refractures of pre-existing fractures may not be detected at all. With the distinction between biconcavity and fracture in this approach, the concept of «vertebral deformity» versus vertebral fracture was introduced. However, it was not expressively attempted to distinguish non-fracture deformities, such as degenerative remodeling, from actual fracture appearances.

Kleerekoper and colleagues (1984) modified Meunier's radiological vertebral index and introduced the "vertebra deformity score" VDS (Nielsen et al. 1991; Olmez et al. 2005), by which each vertebra from T4 to L5 is assigned an individual score from 0 to 3 depending on the type of vertebral deformity. This grading scheme is based on the reduction of the anterior, middle, and posterior vertebral heights, H_a, H_m and H_p, respectively. A vertebral deformity (to be graded 1 to 3) is present when any vertebral height, H_a, H_m, or H_p, is reduced by at least 4 mm or 15%. A vertebral deformity score 0 is assigned to a normal vertebra without any vertebral height reduction. A VDS 1 deformity corresponds to a vertebral end plate deformity with the heights H_a and H_p being normal. A wedge deformity with a reduction of H_a and – to a lesser extent H_m – is assigned a VDS of 2. A compression deformity, which is assigned a VDS of 3, is characterized by a reduction of all vertebral heights H_a, H_m and H_p. Grading all vertebrae T4 to L5 using this score, the minimum VDS for the whole spine would thus be zero with all vertebrae intact and the maximum score would be 42 with compression fractures of all vertebrae. The vertebral deformity score still relies on the type of deformity, i.e., the vertebral shape, and changes of the vertebral shape would be required to account for incident vertebral fractures on follow-up radiographs. A quantitative extension of the VDS with measurements of the vertebral heights accounts for the continuous character of vertebral fractures.

The radiologist's perspective of vertebral fracture diagnosis, i.e., considering the differential diagnosis as well as the severity of a fracture, is probably best reflected in the semiquantitative fracture assessment used in several studies (Genant 1990; Genant et al. 1993). The severity of a fracture is assessed solely by visual determination of the extent of a vertebral height reduction and morphological change, and vertebral fractures are differentiated from other nonfracture deformities. With this approach the type of the deformity (wedge, biconcavity, or compression) is no longer linked to the grading of a fracture as is done with the other standardized visual approaches. Thoracic and lumbar vertebrae from T4 to L4 are graded on visual inspection and without direct vertebral measurement as normal (grade 0), mildly deformed (grade 1, approximately 20%–25% reduction in anterior, middle and/or posterior height and a reduction of 10%–20% of the projected vertebral area), moderately deformed (grade 2, approximately 25%–40% reduction in anterior, middle and/or posterior height and a reduction of 20%–40% of the projected vertebral area), and severely deformed (grade 3, approximately 40% or greater reduction in anterior, middle and/or posterior height and in the projected vertebral area) (Fig. 6.6). From this semiquantitative assessment a "spinal fracture index", SFI, can be calculated as the sum of all grades assigned to the vertebrae divided by the number of the evaluated vertebrae. In addition to height reductions, careful attention is given to alterations in the shape and configuration of the vertebrae relative to adjacent vertebrae and expected normal appearances. These features add a strong qualitative aspect to the interpretation and also render this method less readily definable. Several studies, however, have demonstrated that semiquantitative interpretation, after careful training and standardization, can produce results with excellent intra- and interobserver reproducibility within the same school of training (Genant et al. 1993; Wu et al. 1995).

In a further effort to provide definable, reproducible, and objective methods to detect vertebral fractures and in order to accommodate the assessment of large numbers of radiographs by technicians (in the absence of radiologists or experienced clinicians), various quantitative morphometric approaches

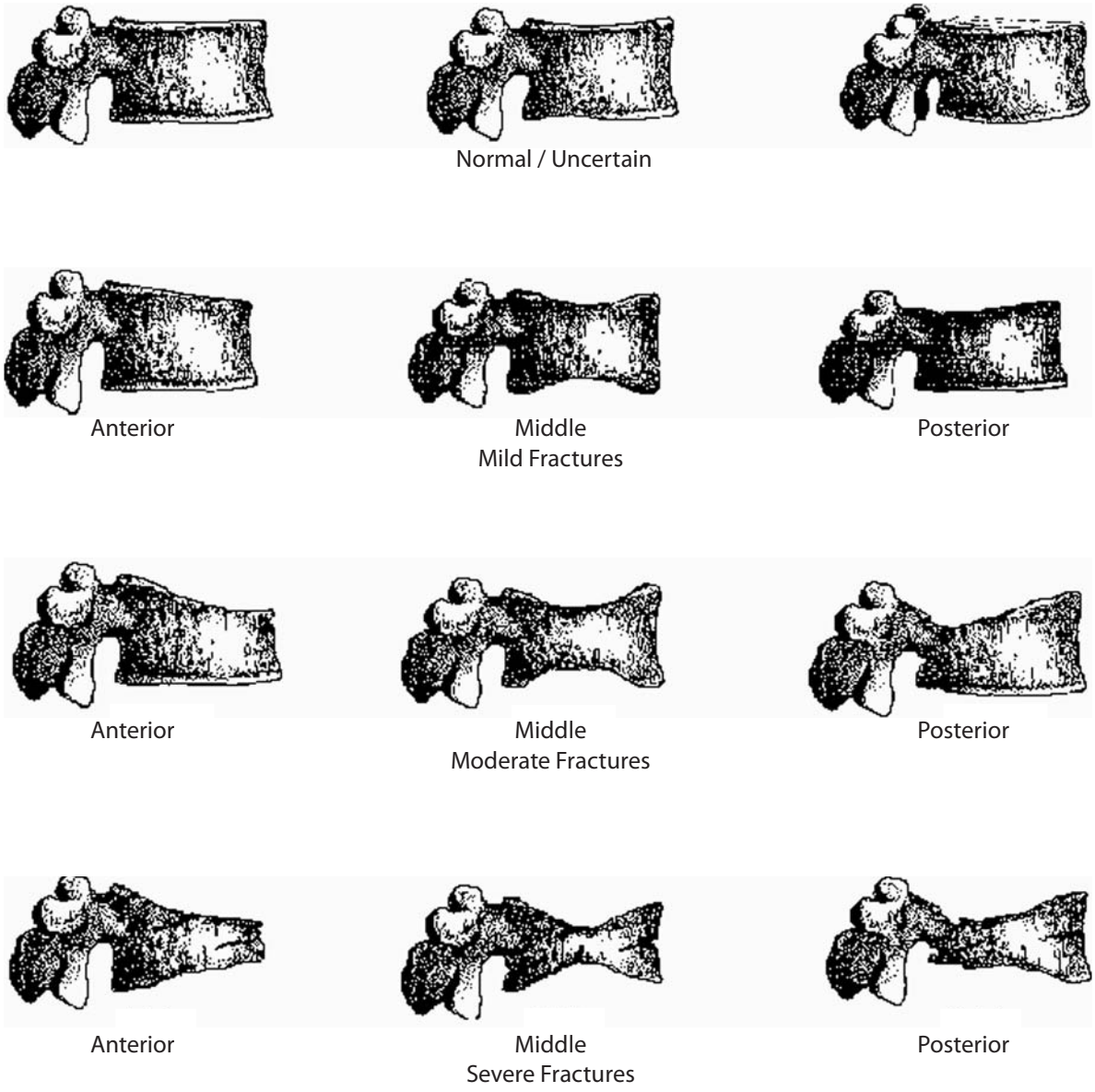

Fig. 6.6. Grading scheme for a semiquantitative assessment of vertebral deformities after Genant. The drawing illustrates the reductions of vertebral height that correspond to the grade of deformity. (Drawing courtesy of Dr. C.Y. Wu)

have been explored and employed. Early studies using direct measurements of vertebral dimensions on lateral radiographs were described by Fletcher in 1946, Hurxthal in 1968, Jensen and Tougaard in 1981, and Kleerekoper et al. in 1984, with the rationale being a reduction in the subjectivity considered intrinsic to the qualitative assessment of spinal radiographs.

Increasingly sophisticated morphometric approaches have been derived for the definition of vertebral dimensions, most of them making 4 to 10 points on a vertebral body to define vertebral heights (Nelson et al. 1990; Spencer et al. 1990; Jergas and San Valentin 1995) (Fig. 6.7). Typically, H_a, H_m and H_p are measured, as is the projected vertebral area. Newer techniques are based on digitally captured conventional radiographs to assess the vertebral dimensions (Kalidis et al. 1992; Evans et al. 1993; Wu et al. 2000). These techniques then rely on either marking points manually to define vertebral heights or finding those points and measuring in an automated or semiautomated fashion.

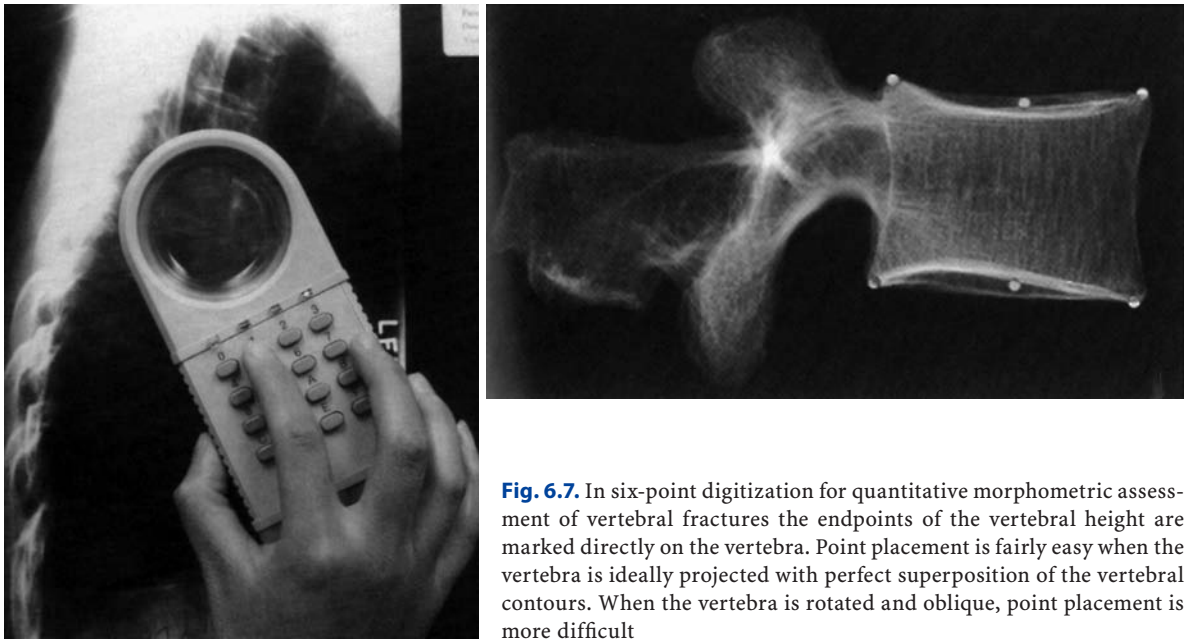

Fig. 6.7. In six-point digitization for quantitative morphometric assessment of vertebral fractures the endpoints of the vertebral height are marked directly on the vertebra. Point placement is fairly easy when the vertebra is ideally projected with perfect superposition of the vertebral contours. When the vertebra is rotated and oblique, point placement is more difficult

Hedlund and Gallagher (1988) used criteria such as percent reduction of vertebral height, wedge angles, and areas in various combinations. Davies and co-workers (1993) employed two distinct morphometric cut-off thresholds for the detection of either vertebral compression or wedge fractures using vertebral height ratios that were defined by a radiologist's assessment of vertebral deformities. Smith-Bindman et al. (1991) initially reported the use of vertebral level specific reductions in anterior, middle, or posterior height ratios expressed as a percentage relative to normal data. Melton et al. (1989) used this level-specific approach, and subsequently Eastell et al. (1991) modified it by applying height ratio reductions in terms of standard deviations rather than percentage. With this approach, each vertebral level has its own specific mean and standard deviation. Minne et al. (1988) developed a method by which vertebral height measures are adjusted according to the height of T4 as a means of standardization, and the resulting values are compared to a normal population. Black et al. (1991) derived a statistical method for establishing normative data from morphometric measures of vertebral heights based upon deletion of the tails of the Gaussian distribution of an unselected population. McCloskey et al. (1993) used vertebral height ratios and introduced an additional parameter defined as a predicted posterior height in addition to the measured posterior height. Ross et al. (1993) further refined morphometric criteria for fracture by utilizing height reductions in standard deviations based on the overall patient specific vertebral dimensions combined with population based level-specific vertebral dimensions.

Several comprehensive studies have compared the various methods or cut-off criteria in the same populations to examine the impact of methodology on estimates of vertebral prevalence and on identification of individual patients or individual vertebrae as fractured. In these studies the expected trade-offs between sensitivity and specificity were observed. Two- to fourfold differences in estimates of fracture prevalence and generally poor or modest kappa scores between the different algorithms for defining fractures were reported (Smith-Bindman et al. 1991; Sauer et al. 1991; Hansen et al. 1992; Adami et al. 1992). Therefore, despite having developed sophisticated, describable, and objective methods, the application and interpretation of the results have been complicated by the large differences observed from one technique to the next. Unfortunately, no true gold standard for defining fractures exists, by which one can judge the methods or their variable cut-off criteria. However, as a first approximation, there is some rationale for comparing visual assessment and morphometric data on a per vertebra basis in order to develop a consensus interpretation based upon the expertise of experienced radiologists and highly trained research assistants (Genant et al.

1996). This may help to understand the reasons for concordant and discordant results and to utilize the strengths of the respective methods. When relying solely on quantitative morphometry one has to consider that no real distinction between osteoporotic fractures and other nonfracture deformities can be made. Besides the uncertainties that are introduced by vertebral projection, differences in the applied technique and intra- and interobserver precision of quantitative morphometry, this may have a substantial impact on the prevalence and to a lesser extent on the incidence of vertebral fractures in a population.

When comparing a standardized visual approach with quantitative morphometry substantial differences between both techniques have been reported, while the agreement between different, centrally trained readers for the semiquantitative approach is reportedly very good (Genant et al. 1993; Wu et al. 1995; Hansen et al. 1992; Leidig-Bruckner et al. 1994). This applies to the diagnosis of both prevalent and incident fractures. Drawing on the strength of each of the approaches both a quantitative approach as well as a standardized visual approach may be applied in combination to reliably diagnose vertebral fractures in clinical drug trials (Genant et al. 1996; Cummings et al. 1995; Grados et al. 2001).

Since dual X-ray absorptiometry is applied in almost all patients suffering from osteoporosis it has been proposed to use this technique to depict the thoracolumbar spine. Initially this technique has been termed morphometric X-ray analysis or MXA (Steiger et al. 1993, 1994). Especially the effect of different projections and magnification effects between two films of the spine will be minimized due to the technical specifications of this technique, and radiation dose may be reduced to a minimum allowing for serial assessment of the fracture status. Since its inception improvements in image quality and the application of refined diagnostic approaches have overcome some of the inherent limitations of the technique such as poor image resolution and relatively high noise levels (Ferrar et al. 2001, 2005) (Fig. 6.8). Since its inception vertebral fracture assessment has been adopted by the major manufacturers of DXA devices, and improvements in image acquisition and vertebral fracture detection have been applied. Depending on the manufacturer, the technique has been termed vertebral fracture assessment (VFA), computer aided fracture assessment (CADfx) or dual energy vertebral assessment (DVA). Several quantitative or semiquantitative techniques may be applied to the acquired scans. The restrictions that are inherent to quantitative morphometry also apply to those scans, potentially even more since image quality does not always warrant a thorough diagnostic evaluation of a vertebral deformity. While vertebral fracture detection may be helpful in the serial assessment of vertebral deformities and it is now widely applied, its diagnostic validity still requires thorough evaluation by the experienced technologist and physician (Chappard et al. 1998; Ferrar et al. 2000; Rea et al. 2000; Guermazi et al. 2002; Jacobs-Kosmin et al. 2005). Vertebral fracture assessment in its present form is an effective tool to identify moderate and severe vertebral deformities (Schwartz and Steinberg 2005). Thus, VFA may serve as a valuable tool for the identification of high-risk patients and as a screening tool for clinical trials.

Fig. 6.8a,b. The lateral assessment of vertebral deformities using a dual energy X-ray absorptiometry scanner is termed vertebral fracture assessment (VFA). The resulting image of the spine allows for a morphometric analysis of vertebral deformities as well as an identification of vertebral fractures using a semiquantitative technique

6.2.2.1 Osteopenia and Osteoporosis at Other Skeletal Sites

The axial skeleton is not the only site where characteristic changes of osteopenia and osteoporosis can be depicted radiographically. Changes in the trabecular and cortical bone can also be seen in the appendicular skeleton. It is first apparent at the ends of long and tubular bones due to the predominance of cancellous bone in these regions. Endosteal resorption has a prominent role particularly in senile osteoporosis. The net result of this chronic process is widening of the medullary canal and thinning of the cortices. In late stages of senile osteoporosis, the cortices are paper-thin and the endosteal surfaces are smooth. In rapidly evolving postmenopausal osteoporosis accelerated endosteal and intracortical bone resorption may be seen and can be directly assessed by high-resolution radiographic techniques. Methods to quantitate the changes at the peripheral skeleton have been proposed and also clinically applied (e.g., Singh index, radiogrammetry) (Singh et al. 1970; Barnett and Nordin 1961; Meema and Meema 1981). Conventional radiography is the basis for a number of recent studies exploring new aspects of assessing bone structure using sophisticated image analysis procedures such as fractal analysis or fast Fourier transforms (Benhamou et al. 1994; Geraets et al. 1998; Link et al. 1997; Lespessailles et al. 1998). These techniques have also been applied to the study of bone structure using high resolution images acquired with magnetic resonance imaging or computed tomography in a research setting (Majumdar et al. 1998, 1999; Millard et al. 1998; Link et al. 1998; Laib and Ruegsegger 1999; Cortet et al. 1999).

6.2.3 Differential Diagnosis of Reduced Bone Mass

Aside from senile and postmenopausal states there are various other conditions that may be accompanied by generalized osteoporosis. While most of the previously mentioned radiographic characteristics are shared by a variety of conditions, there may be some apparent differences in the appearance of osteoporosis as compared to involutional osteoporosis.

6.2.3.1 Endocrine Disorders Associated with Osteoporosis

Increased serum concentrations of parathyroid hormone in hyperparathyroidism may result from autonomous hypersecretion by a parathyroid adenoma or diffuse hyperplasia of the parathyroid glands (primary hyperparathyroidism). A long sustained hypocalcaemic stimulus may result in hyperplasia of all parathyroid glands and secondary hyperparathyroidism (Fig. 6.9). The cause of hypocalcaemia usually is chronic renal failure or rarely malabsorption states. Patients with long-standing hyperparathyroidism may develop autonomous function and hypercalcaemia (tertiary hyperparathyroidism). While it is the increase in serum parathyroid hormone and calcium that establishes the diagnosis, radiographs document the severity and course of the disease. Hyperparathyroidism leads to both increased bone resorption and bone formation. Changes induced by hyperparathyroidism may affect all bone surfaces resulting in subperiosteal, intracortical, endosteal, subchondral, subepiphyseal, subligamentous, subtendinous and trabecular bone resorption (Genant et al. 1973, 1974; Richardson et al. 1986).

Subperiosteal bone resorption is the most characteristic radiographic feature of hyperparathyroidism (Camp and Ochsner 1931). It is especially prominent in the hand, wrist and foot but may also be seen other sites. Radiographically, the outer margin of the bone becomes indistinct. Scalloping and spiculations of the cortex may occur in later stages.

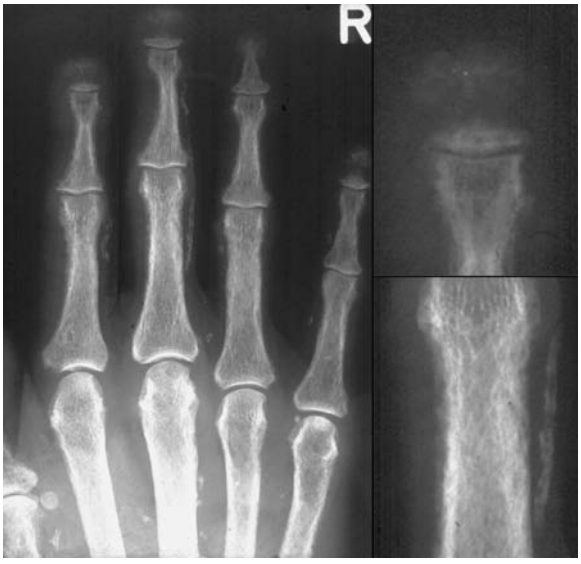

Fig. 6.9. Conventional radiograph of the hand in secondary hyperparathyroidism. The magnification illustrates periosteal bone resorption with indistinct delineation of the outer cortical border. There is also osteolytic appearance of the distal phalanges due to undermineralization of the osseous substance

Undermineralization of the tela ossea leads to the distinctive radiographic appearance of acro-osteolyses (Resnick and Niwayama 1995). Intracortical resorption results in longitudinally oriented linear striations within the cortex (cortical tunneling), and endosteal bone resorption leads to scalloping of the inner cortex, cortical thinning and widening of the medullary canal (Meema and Meema 1972). Cortical tunneling is nonspecific and may be seen in other diseases of rapid bone turnover, including hyperthyroidism, reflex sympathetic dystrophy, acute disuse osteoporosis and Paget's disease.

Subchondral bone resorption frequently also affects the joints of the axial skeleton causing undermineralization of the Tela ossea. For example, it may mimic widening of the sacroiliac joint space leading to 'pseudo-widening' of the joint (Hayes and Conway 1991). The osseous surface may collapse, and thus may simulate subchondral lesions of inflammatory disease. Osteopenia occurs frequently in hyperparathyroidism and may be observed throughout the skeleton. Other radiographic signs of hyperparathyroidism include focal bone lesions ("brown tumors"), cartilage calcification resulting from the deposition of of calcium pyrophosphate dehydrate crystals (CPPD) and also bone sclerosis (Steinbach et al. 1961). Increased amounts of trabecular bone leading to bone sclerosis may occur especially in patients with renal osteodystrophy and secondary hyperparathyroidism. Increased bone density may occur preferably in the axial skeleton, sometimes leading to deposition of bone in subchondral areas of the vertebral body resulting in an appearance of radiodense bands across the superior and inferior border and normal or decreased density of the center ("rugger-jersey spine") (Resnick 1981).

While osteoporosis is defined by a reduction of regularly mineralized osteoid, findings in osteomalacia include an abnormally high amount of non-mineralized osteoid, and a reduction in mineralized bone volume. Thus, radiographic abnormalities in osteomalacia include osteopenia (reduction of mineralized bone), coarsened, indistinct trabeculae and unsharp delineation of cortical bone (excessive apposition of non-mineralized osteoid), deformities, insufficiency fractures and true fractures (bone softening and weakening) (Reginato et al. 1999). Deformations include bowing and bending of the long bones, and biconcave deformities of the vertebrae (Kienböck 1940). Pseudofractures, or Looser's zones (focal accumulations of osteoid in compact bone at right angles of the long axis), are diagnostic of osteomalacia and often occur bilateral and symmetrical. There are more than 50 different diseases that may cause osteomalacia of which chronic renal insufficiency, hemodialysis and renal transplantation are the most common causes (Pitt 1991; Kainberger et al. 1992). Modern patient management has resulted in typical radiographic features of osteomalacia being present in only a minority of these patients (Adams 1999). A decrease of vitamin D and reduced responsiveness in chronic renal insufficiency leads to osteomalacia and rickets. The additional secondary hyperparathyroidism leads to a superimposition of radiographic changes from both osteomalacia and secondary hyperparathyroidism (Sundaram 1989). This radiographic appearance is termed renal osteodystrophy. A common finding in secondary hyperparathyroidism associated with renal osteodystrophy is the osteosclerosis resulting in typical appearance of the vertebral bodies as seen in the rugger-jersey spine (Pitt 1991). Several other radiographic abnormalities may be frequently seen in renal osteodystrophy (Fig. 6.10) including amyloid deposits, destructive spondyloarthropathy, inflammatory changes, and avascular necrosis, soft tissue calcification and arteriosclerosis (Kriegshauser et al. 1987; Murphey et al. 1993).

Hyperthyroidism is a high-turnover disease, and it is associated with an increase in both bone resorption and bone formation (Mosekilde et al. 1990). Since bone resorption exceeds bone formation rapid bone loss may occur and result in generalized osteoporosis with the largest effect on cortical bone (Greenspan and Greenspan 1999). This effect is especially pronounced in patients with thyrotoxicosis, or with a history of thyrotoxicosis (Toh et al. 1985). TSH-suppressive doses of thyroid hormone have been reported to decrease, or have no effect on bone density (Nuzzo et al. 1998). Radiological findings of hyperthyroidism-induced osteoporosis are those that are commonly seen in involutional or senile osteoporosis including generalized osteopenia and cortical thinning and tunneling. The fractures associated with this condition affect the spine, the hip, as well as the distal radius (Chew 1991; Solomon et al. 1993).

6.2.3.2 Medication-Induced Osteoporosis

Hypercortisolism is probably the most common cause of medication induced generalized osteoporo-

Fig. 6.10. Renal osteodystrophy presenting with increased sclerosis of the vertebral endplates. There is a vertebral fracture in the upper thoracic spine leading to increased kyphosis

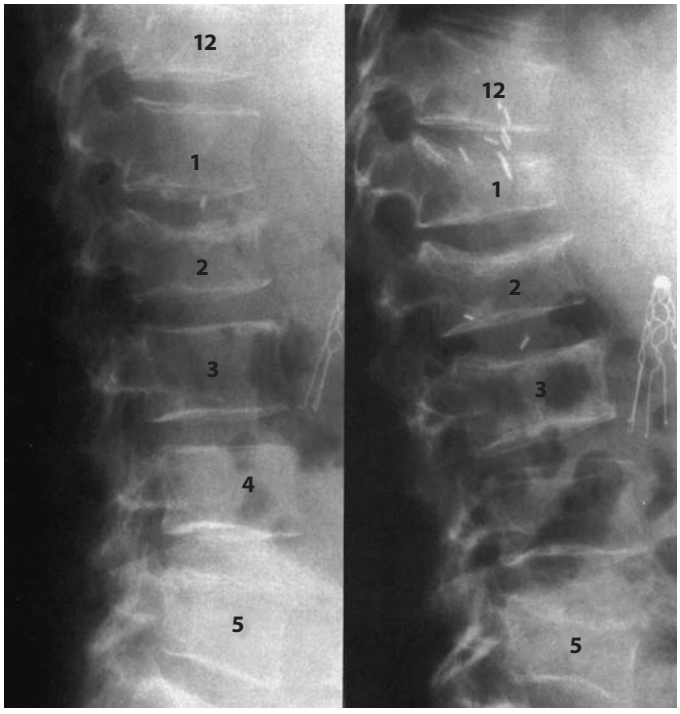

Fig. 6.11. Serial radiographs in heparin-induced osteoporosis. The follow-up radiograph (*right*) reveals newly developed fractures of the 1st, 3rd and 5th lumbar vertebrae

sis while the endogenous form of hypercortisolism, Cushing's disease, is relatively rare (Laan et al. 1993; Saito et al. 1995; Adachi et al. 1993). That is why this form of osteoporosis is listed in this section on medication-induced osteoporosis. Decreased bone formation and increased bone resorption have been observed in hypercortisolism. This has attributed to inhibition of osteoblast formation, either direct stimulation of osteoclast activity or increased secretion of parathyroid hormone. The typical radiographic appearance of steroid-induced osteoporosis comprises generalized osteoporosis, at predominantly trabecular sites, with decreased bone density and fractures of the axial but also of the appendicular skeleton. A characteristic finding in steroid-induced osteoporosis is the marginal condensation of the vertebral bodies resulting from exuberant callus formation. Avascular osteonecrosis is another complication of hypercortisolism, most frequently involving the femoral head, and to a lesser extent the humeral head and the femoral condyles (Heimann and Freiberger 1969; Hurel and Kendall-Taylor 1997). Unlike the avascular osteonecrosis of joints, these bone marrow infarcts are clinically silent and insignificant.

Generalized osteoporosis has been observed in patients receiving high dose heparin therapy (Griffith et al. 1965; Rupp et al. 1982; Nelson-Piercy 1998) (Fig. 6.11). The radiological features of heparin-induced osteoporosis include generalized osteopenia and vertebral compression fractures (Sackler and Liu 1973). The pathomechanism of heparin-induced osteoporosis is not completely clear, and there may be a prolonged effect on bone even after cessation of therapy (Walenga and Bick 1998; Shaughnessy et al. 1999).

6.2.3.3 Other Causes of Generalized Osteoporosis

Other causes of generalized osteoporosis include malnutrition, chronic alcoholism (if associated with malnutrition), smoking and caffein intake, Marfan syndrome and, somewhat infrequently, pregnancy (Seeman et al. 1992; Kohlmeyer et al. 1993; Smith et al. 1985; Hopper and Seeman 1994; Diez et al. 1994). Marrow abnormalities associated with osteoporosis are anemias (sickle cell anemia, thalassemia), plasma cell myeloma, leukemia, Gaucher's disease and glycogen storage disease (Resnick

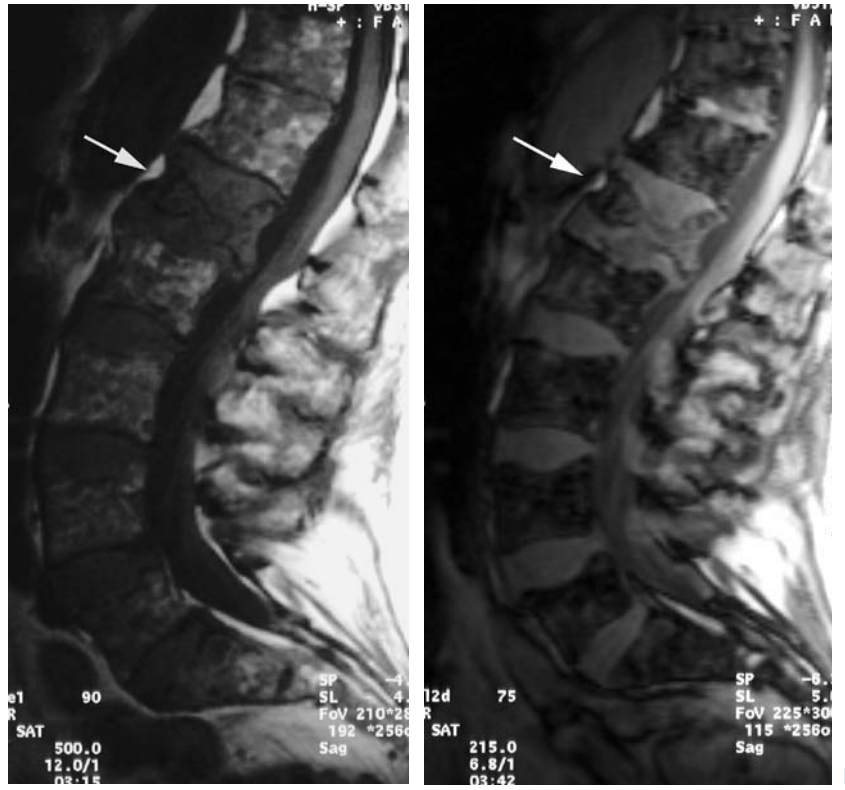

a b

Fig. 6.12a,b. Multiple myeloma often cannot be distinguished from osteoporosis on conventional radiographs. Magnetic resonance imaging often reveals the bone marrow involvement and makes it possible to distinguish multiple myeloma from osteoporosis. In this patient with multiple myeloma, extensive inhomogeneities ("salt and pepper") of the bone marrow signal can be seen on T1-weighted images suggesting the nature of the disease as well as the extent of bone marrow involvement. There is a fracture of L1

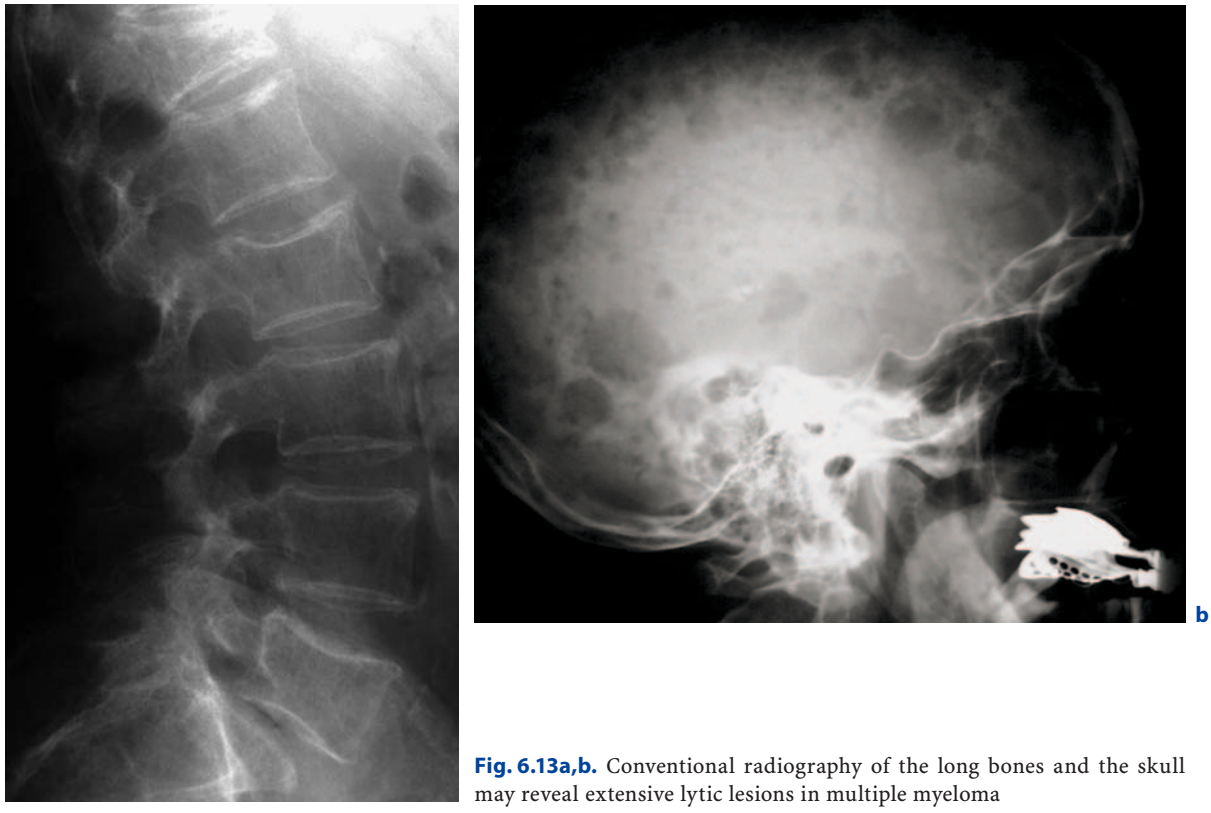

a b

Fig. 6.13a,b. Conventional radiography of the long bones and the skull may reveal extensive lytic lesions in multiple myeloma

1995a,b) (Fig. 6.12, Fig. 6.13). This list is certainly far from being complete but it represents some of the major causes of osteoporosis. Additional imaging techniques such as computed tomography, magnetic resonance tomography and bone scintigraphy, as well as clinical information, may be helpful in the differential diagnosis of the various conditions associated with osteoporosis (Stäbler et al. 1996; Baur et al. 1998; Moulopoulos and Dimopoulos 1997; Lecouvet et al. 1997a,b).

There are some conditions of the juvenile skeleton that result in generalized osteoporosis. Rickets is characterized by inadequate mineralization of the bone matrix, and some of its radiographic appearance may resemble that of osteomalacia (Molpus et al. 1991). Widening of the growth plates, cupping of the metaphysis, and decreased density and irregularities of the metaphyseal margins may be present (Pitt 1995). Epiphyseal ossification centers may show delayed ossification and unsharp borders (Steinbach et al. 1954). Overgrowth of the hyaline cartilage may lead to prominence of costochondral junctions of the ribs (rachitic rosary). The child's age at the onset of the disease determines the pattern of bone deformity, with bowing of the long bone being more pronounced in infancy and early childhood, and vertebral deformities and scoliosis in older children (Rosenberg 1991). Further deformities that may be observed in rickets include pseudofractures, basilar invagination and triradiate configuration of the pelvis.

Idiopathic juvenile osteoporosis is a self-limited disease of childhood with recovery occurring as puberty progresses (Smith 1995). A typical feature of this condition is the increased vulnerability of the metaphyses, often resulting in metaphyseal injuries of the knees and ankles. Idiopathic juvenile osteoporosis must be distinguished from osteogenesis imperfecta, another disease often presenting with radiographic signs of generalized osteoporosis (Smith 1995). The pathogenesis of osteogenesis imperfecta is quantitative or qualitative abnormalities of type I collagen. There are four major types of osteogenesis imperfecta, and the degree of osteoporosis in osteogenesis imperfecta depends strongly on the type of disease (Minch and Kruse 1998). The clinical features of each type usually correspond to the type of mutation. The abnormal maturation of collagen seen in this disorder results in a primary defect in bone matrix. This, combined with a defective mineralization, result in overall loss of bone density involving both the axial and peripheral skeleton. Patients with type III disease have a significantly decreased bone density presenting with generalized osteopenia, thinned cortices, fractures of long bones and ribs, exuberant callus formation and bone deformation (Hanscom et al. 1992). The degree of osteopenia is highly variable, however, and at the mildest end of the spectrum some patients do not have any radiographic signs of osteopenia (Zionts et al. 1995).

6.3 Regional Osteoporosis

Osteoporosis may also be confined to only a segment of the body. This type of osteoporosis is called regional osteoporosis, and it is commonly caused by some disorder of the appendicular skeleton. Osteoporosis due to immobilization or disuse characteristically occurs in the immobilized regions of patients with fractures, motor paralysis due to central nervous system disease or trauma and bone and joint inflammation (Kiratli 1996). Chronic and acute disease may vary in their radiographic appearance somewhat, showing diffuse osteopenia, linear radiolucent bands, speckled radiolucent areas and cortical bone resorption.

Reflex sympathetic dystrophy, sometimes also termed Sudeck's atrophy or algodystrophy, has the radiographic appearance of a high turnover process. It most often occurs in patients with trauma, such as Colles' fracture but also in patients with any neurally related musculoskeletal, neurologic, or vascular condition such as hemiplegia or myocardial infarction (Sudeck 1901; Oyen et al. 1993; Sarangi et al. 1993). This condition is probably related to overactivity of the sympathetic nervous system with increased blood flow and increased intravenous oxygen saturation in the affected extremity (Gellman et al. 1992; Schwartzman and McLellan 1987). Its radiographic appearance includes soft tissue swelling as well as regional osteoporosis showing with bandlike, patchy, or periarticular osteoporosis. Additional radiographic features include subperiosteal bone resorption, intracortical tunneling, endosteal bone resorption with initial excavation and scalloping of the endosteal surface and subsequent remodeling and widening of the medullary canal, as well as subchondral and juxtaarticular erosions (Resnick and Niwayama 1995). Especially in the

early stages of reflex sympathetic dystrophy, bone scintigraphy may be helpful to establish the diagnosis (Todorovic Tirnanic et al. 1995; Leitha et al. 1996).

Transient regional osteoporosis includes conditions that have in common the development of self-limited pain and radiographic osteopenia affecting one or several joints, most commonly the hip. Transient osteoporosis typically occurs in middle-aged men and women in the third trimester of pregnancy. At the onset of clinical symptoms, there may be normal radiographic findings, and within several weeks, patients develop variable osteopenia of the hip, sometimes involving the acetabulum. Some patients later develop similar changes in the opposite hip or in other joints, in which case the term regional migratory osteoporosis may be used. The cause of transient regional osteoporosis is not known, and it appears that it may be related to reflex sympathetic dystrophy. In some patients with clinically similar or identical manifestations, magnetic resonance imaging presents with transient regional bone marrow edema (Hayes et al. 1993; Boos et al. 1993). Since not all patients with identical clinical symptoms and transient bone marrow edema develop regional osteoporosis, the sensitivity as to the detection of regional osteoporosis has to be questioned as well as the interrelationship between transient regional osteoporosis and transient bone marrow edema (Palit et al. 2006). There also seems to be a relationship of transient bone marrow edema to ischemic necrosis of bone, and there is a need to define criteria for allowing differentiation of transient bone marrow edema and the edema pattern associated with osteonecrosis (Trepman and King 1992; Froberg et al. 1996; Guerra and Steinberg 1995; Gil et al. 2006).

6.4 Quantifying Bone Mineral in Conventional Radiography

6.4.1 Standardized Evaluation of Conventional Radiographs

The lack of methods to objectively assess bone density in the past made some researchers use the characteristic radiographic appearance of bone in osteoporosis to grade or classify osteoporosis, e.g., Saville's score (Saville 1967). Doyle and coworkers (1967) studied radiological criteria of osteoporosis and found, with the exception of biconcavity, none of the other criteria to be valid criteria for the diagnosis of osteoporosis. For follow-up even increased biconcavity was not a useful criterion. 'Can Radiologists Detect Osteopenia on Plain Radiographs?' Garton and colleagues (1994) asked and concluded that even though the reproducibility of Saville's score was only moderate, bone density was significantly correlated with this score. Potentially, aside from single criteria, the radiographic impression of the spine as a whole may hint to a reduced bone density (Ahmed et al. 1998). Therefore, and because it is essential for differential diagnosis of osteoporosis and for the diagnosis and follow-up of vertebral deformities, conventional radiography will remain an important asset to the diagnosis of osteoporosis.

In an attempt to quantitate the degree of osteoporosis, Barnett and Nordin (1960, 1961), and in a similar form Dent and colleagues (1953), proposed that the increased biconcavity of a vertebra could be used to diagnose and follow osteoporosis. The quotient of middle and anterior vertebral height today is associated with the names of Barnett and Nordin. However, the authors only used one vertebra to calculate their score (usually L3) which may not represent the bone mineral status of the whole spine (Jergas et al. 1994). Furthermore, following the course of osteoporosis using only one vertebra may also be regarded as problematic.

Urist (1960) reported that in women with hip fracture the principal compressive trabeculae in the proximal femur become more prominent while other groups of trabeculae are resorbed. Based on this observation in women with advanced osteoporosis Singh et al. (1970) proposed a femoral index for the diagnosis of osteoporosis based on the assumption that the trabeculae in the proximal femur disappear in a predictable sequence depending on their original thickness (Fig. 6.14). The authors considered that the thickness and spacing of trabeculae in the various trajectorial groups (principal compressive, secondary compressive, greater trochanter, principal tensile, and secondary tensile group) depend on the intensity of stresses normally carried by these trabeculae. With advancing bone loss trabeculae that are thinner become invisible first on the radiograph. Singh and coworkers (1970) introduced a classification rang-

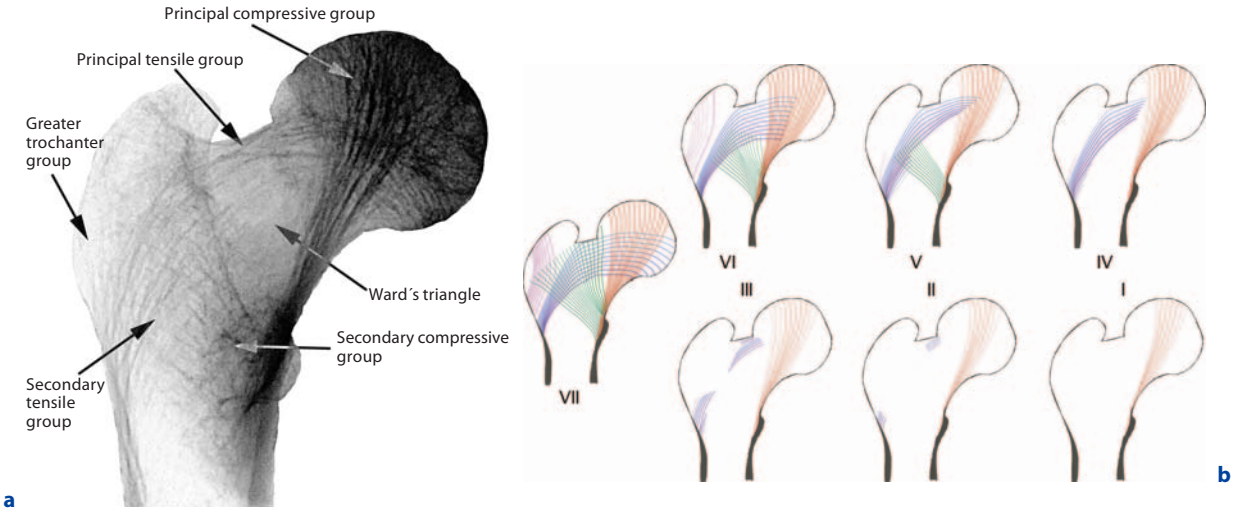

Fig. 6.14a,b. The Singh index is based on the assumption that the trabeculae in the proximal femur (**a**) disappear in a predictable sequence depending on their original thickness. The classification ranges from grade VII (normal, all trabecular groups visible) to grade I (marked reduction of even the principal compressive trabeculae) according to the degree of bone loss (**b**)

ing from grade VI (normal, all trabecular groups visible) to grade I (marked reduction of even the principal compressive trabeculae) according to the degree of bone loss. Singh et al. (1972) later added a grade VII to their scale for individuals with dense bone, meaning that the Ward's triangle (an area on radiographs of the proximal femur enclosed by the principle and secondary compressive, and the tensile groups) contained trabeculae that were as dense as the other surrounding trabeculae. The authors reported a relatively good discrimination of individuals with and without vertebral fractures. Interobserver variation for the Singh index is highly variable being influenced strongly by the quality of the radiographs, the degree of osteoporosis (moderate changes being harder to agree on than on the extremes), and the experience of the observer. Right-left comparisons of the Singh index show a concordance on the order of 80%. The Singh index has been applied in a number of studies in which varying results in the relationship to bone mass and vertebral appearance have been shown (Griffiths and Virtama 1990; Peacock et al. 1995; Koot et al. 1996). More recent observations indicate that the underlying assumption of the Singh index, the organized sequential loss of trabeculae, may be false and a generalized loss of bone mineral in both the tensile and compressive occurs. A similar grading scheme for estimating bone loss exists for the calcaneus (Jhamaria et al. 1983).

6.4.2 Radiogrammetry

Radiogrammetry, a simple measurement of cortical thickness in virtually any tubular bone, is easy to perform with a caliper or with a graduated magnifying glass. Simple cortical measurements may be represented in several ways (Fig. 6.15): One method involves summing the thickness of both cortices as an index of bone mass; another method uses the combined cortical thickness divided by the total bone width as a measure of density; finally, a circular cross-section of bone can be assumed with the measurements of bone width and cortical thickness converted to cortical areas that more closely parallel actual physical mass. Radiogrammetry is applied most often to the metacarpal bones (Kalla et al. 1989). The use of a caliper, the combination of a number of metacarpals or repeated measurements of one metacarpal and the use of digitization techniques or automated edge detection on digitally acquired radiographs may improve the precision error (Horsman and Simpson 1975; Bloom et al. 1983; Rico and Hernandez 1989). Variations in soft tissue thickness and in radiographic geometry cause systematic errors. As a consequence of these inaccuracies and the imprecision of the measurements, the values for compact bone area derived from radiogrammetry at different skeletal locations are correlated only moderately. The correlation between right-

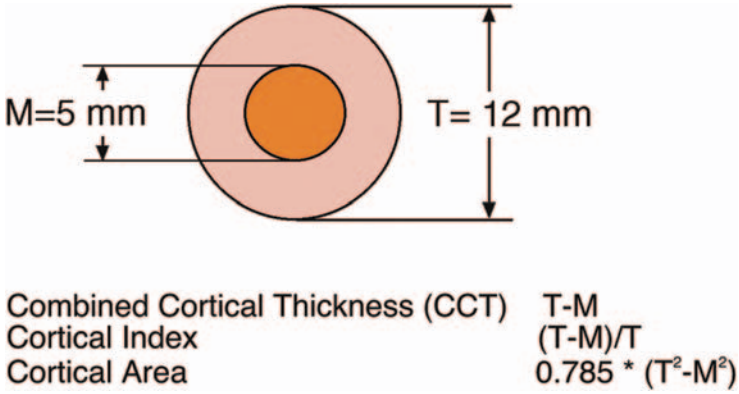

a

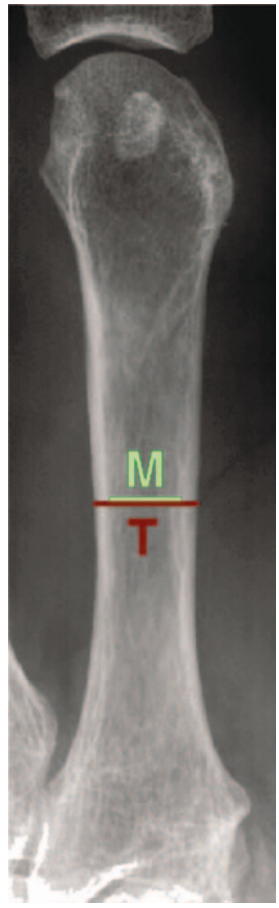

b

Fig. 6.15a,b. For a long time radiogrammetry represented the only quantitative method to evaluate changes of bone density by measuring the thickness of the cortical bone. The results may be expressed as combined cortical thickness, cortical index, or even an assumed cortical area. Typically, this measurement is performed on the second metacarpal bone

and left-sided bones is higher (Helela and Virtama 1970; Bloom 1980; Plato and Purifoy 1982). While Meema and Meindok (1992) reported a good correlation between radiogrammetric measurements and dual photon absorptiometry of the spine, other studies suggest only a poor to moderate correlation with other methods of bone mineral measurements (Guesens et al. 1986; Rosenthal et al. 1987).

Simple cortical measurements, particularly when obtained at several anatomic sites, provide information that is more useful in clinical research than in individual patient management. For example, extensive data on metacarpal changes in populations show a loss with aging in men and women (Geusens et al. 1986; Dequeker 1976; Evans et al. 1978; Garn et al. 1967; Falch and Sandvik 1990; Maggio et al. 1997). Studies of patients with primary hyperparathyroidism, rheumatoid arthritis and systemic lupus erythematosus have revealed substantial reductions of the combined cortical thickness compared to normal controls (Genant et al. 1973; Kalla et al. 1992). Meema (1991) and Meema and Meema (1987) found radiogrammetry to be a good discriminator between postmenopausal women with and without vertebral fractures. While the aforementioned studies all used radiogrammetry on plain films, Crespo and colleagues (1998) reported on the use of computed tomography for the determination of cortical area. The authors found that cortical bone loss was associated with prevalent Colles' fractures in postmenopausal women.

A variation of radiogrammetry was introduced a few years ago and is called digital X-ray radiogrammetry, or DXR. In this technique a radiogram of the hand or forearm is scanned with a commercial high-resolution scanner, and the digital image of the forearm is analyzed using various regions of interest in three metacarpals II to IV. A BMD equivalent DXR bone density is calculated from cortical thickness of these bones and image procession algorithms are applied to calculate additional parameters, striation and porosity (Malich et al. 2004). Initial results

showed the method provided adequate precision as well as a good association with age and with the history of fracture (Jorgensen et al. 2000; Toledo and Jergas 2006). In the context of the large epidemiological 'Study of Osteoporotic Fractures' digital radiogrammetry proved to be predictive of incident fractures of the wrist, hip and spine (Bouxsein et al. 2002).

One major limitation of radiogrammetry is its failure to measure intracortical resorption or porosity and irregular endosteal scalloping or erosion. As intracortical and trabecular bone resorptions are important indicators of high bone turnover states, the fact that they are not measured by this technique is significant. Despite its shortcomings when applied to individual patients, radiogrammetry remains an important research tool, especially for studying changes in cortical bone (van Rijn et al. 2004, 2006; Goerres et al. 2007; Bottcher et al. 2005).

6.4.3 Photodensitometry or Radiographic Absorptiometry (RA)

It has been known for many years that the photographic density on a film is roughly proportional to the mass of bone located in the X-ray beam. A relatively large change in bone mineral content (25%–50%) must occur, however, before it can be detected with visual observation of radiographs (Lachmann and Whelan 1936; Virtama 1960). Some investigator proposed to include a standard bone on an the X-ray of the hand, or even with a spine radiograph (Steven 1947; Nordin et al. 1962). In an effort to quantitate bone mass, a number of investigators have measured the optical density of bone contained in radiographs, in which both the anatomic part to be studied and a reference wedge are included in the exposure area (Hodge et al. 1935; Stein 1937; Mack et al. 1939; Cosman et al. 1991; Trouerbach et al. 1987) (Fig. 6.16). The simultaneous exposure of a reference system (usually a wedge or step wedge consisting of aluminum or hydroxyapatite) allows for a reproducible determination of bone density with an appropriate exposure technique. Following film processing, bone and reference wedge are evaluated using a photo densitometer. In its long history, many names have been assigned to this technique like radiographic photodensitometry, radiographic absorptiometry, quantitative Röntgen microdensitometry, and even digital image processing. They are all basically the same technique using more or less sophisticated approaches.

Photodensitometry is a low dose and low cost technique, which measures integral bone (trabecular and cortical). Moreover, photodensitometry is easy to perform. Multiple technical problems arise, however, such as nonuniformity of X-ray intensity beam hardening due to the polychromatic radiation source, and variation in film sensitivity related to processing. Photodensitometry is limited to the peripheral skeleton because of soft tissue inhomogeneities. Various measurement sites in the upper and lower extremities are reported in the literature. Metacarpal or phalangeal bones are preferred sites. Heuck and Schmidt (1960) reported an accuracy of 5%–10% for photodensitometry of the femoral neck and the calcaneus. Some results using more advanced photodensitometric techniques suggest that precision on the order of 1%–3.5% for photodensitometry of the phalangeal or metacarpal bones is possible (Trouerbach et al. 1987; Hayashi et al. 1990; Meema and Meema 1969).

Fig. 6.16. In radiographic absorptiometry the simultaneous exposure of a reference system (usually a wedge or step wedge consisting of aluminum or hydroxyapatite) enables the reproducible determination of bone density with an appropriate exposure technique. By comparing the attenuation values of the reference with known density values one determines corresponding density of a region of interest in the bone

Hagiwara et al. (1993) found the correlation coefficient between photodensitometry of the metacarpal bones and their ash density to be r = 0.95 (CV% = 3.4%). Results derived from photodensitometry of the hand compared significantly with other bone density measurements in vivo. Moderate correlation coefficients between spinal BMD using a dual photon absorptiometry technique and photodensitometry of the hand were reported. The correlation with other measurement sites was found to be in the same order (Cosman et al. 1991).

The early investigations of Meema and Meema (1976) showed that, at all ages, women have less cortical bone than men and that age-related bone loss starts earlier, proceeds more rapidly, and results in a much greater depletion of the skeleton in women than in men (Trouerbach et al. 1987, 1993). Several investigators have studied the association between BMD of the phalanges assessed by radiographic absorptiometry and fracture risk in cross-sectional studies. Here the significant relationship with prevalent vertebral fractures could be confirmed (Ross et al. 1995; Takada et al. 1997; Hagiwara et al. 1998; Versluis et al. 2000). Mussolino et al. (1997) examined the relationship between phalangeal bone density in women and future hip fracture risk using prospective fracture data with a maximum follow-up of 16 years from the NHANES I study. They found a significant association between phalangeal bone density at baseline and future hip fractures with an age-adjusted relative risk of approximately 1.8 per 1 standard deviation decrease in bone mass. These results for the female study cohort could also be confirmed in the male NHANES study cohort (Mussolino et al. 1998). However, in a cross-sectional study Ekman and colleagues (2001) found that neither quantitative ultrasound nor densitometry of the phalanges could discriminate between women with and without hip fracture. As a plus, cost effectiveness, ease of use and its theoretically ubiquitous availability make this technique an interesting option for the assessment of bone mass. Nevertheless, the value of peripheral measurements for the diagnosis of osteoporosis and the prediction of the significant hip fractures and vertebral fractures have to be studied further.

Even some of the methods used to study bone density at the axial skeleton are derived from radiographic absorptiometry. Classic photodensitometry cannot be applied to the axial skeleton due to the greater amount and inhomogeneity of the surrounding soft tissue. Krokowski and Schlungbaum already reported on a photodensitometric method for determining the bone mineral content at the lumbar spine in 1959. The authors used two lateral radiographs of the lumbar spine taken at two distinct energies (62 and 250 kV) to calculated bone density in a region of interest (Krokowski and Schlungbaum 1959). This method described the basic principles of what was to become the most widespread technique to assess bone density at the axial skeleton, dual photon or X-ray absorptiometry (DPA, DXA).

References

Adachi JD, Bensen WG, Hodsman AB (1993) Corticosteroid-induced osteoporosis. Semin Arthr Rheum 22:375–384

Adami S, Gatti D, Rossini M, Adamoli A, James G, Girardello S, Zamberlan N (1992) The radiological assessment of vertebral osteoporosis. Bone 13[Suppl]:S33–S6

Adams JE (1999) Renal bone disease: radiological investigation. Kidney Int Suppl 73:S38–S41

Ahmed AIH, Ilic D, Blake GM, Rymer JM, Fogelman I (1998) Review of 3530 referrals for bone density measurements of spine and femur: evidence that radiographic osteopenia predicts low bone mass. Radiology 207:619–624

Albright F(1947) Osteoporosis. Annals of internal medicine. 27:861–882

Albright F, Smith PH, Richardson AM (1941) Postmenopausal osteoporosis. Its clinical features. JAMA 116:2465–2474

Ballock RT, Mackersie R, Abitbol JJ, Cervilla V, Resnick D, Garfin SR (1992) Can burst fractures be predicted from plain radiographs? J Bone Joint Surg [Br] 74:147–150

Barnett E, Nordin BEC (1960) The radiological diagnosis of osteoporosis: a new approach. Clin Radiol 11:166–174

Barnett E, Nordin BEC (1961) Radiological assessment of bone density. I. The clinical and radiological problem of thin bones. Br J Radiol 34:683–692

Baur A, Stäbler A, Steinborn M, Schnarkowski P, Pistitsch C, Lamerz R, Bartl R, Reiser M (1998) Magnetresonanztomographie beim Plasmozytom: Wertigkeit verschiedener Sequenzen bei diffuser und lokaler Infiltrationsform. RöFo Fortschr Röntgenstr 168:323–329

Benhamou CL, Lespessailles E, Jacquet G, Harba R, Jennane R, Loussot T, Tourliere D, Ohley W (1994) Fractal organization of trabecular bone images on calcaneus radiographs. J Bone Miner Res 9:1909–1918

Black DM, Cummings SR, Stone K, Hudes E, Palermo L, Steiger P (1991) A new approach to defining normal vertebral dimensions. J Bone Miner Res 6:883–892

Bloom RA (1980) A comparative estimation of the combined cortical thickness of various bone sites. Skeletal Radiol 5:167–170

Bloom RA, Pogrund H, Libson E (1983) Radiogrammetry of the metacarpal: a critical reappraisal. Skeletal Radiol 10:5–9

Boos S, Sigmund G, Huhle P, Nurbakhsch I (1993) Magnetresonanztomographie der sogenannten transitorischen Osteoporose. Primärdiagnostik und Verlaufskontrolle nach Therapie. Röfo Fortschr Geb Rontgenstr Neuen Bildgeb Verfahr 158:201–206

Böttcher J, Pfeil A, Rosholm A, Petrovitch A, Seidl BE, Malich A, Schäfer ML, Kramer A, Mentzel HJ, Lehmann G, Hein G, Kaiser WA (2005) Digital X-ray radiogrammetry combined with semiautomated analysis of joint space widths as a new diagnostic approach in rheumatoid arthritis: a cross-sectional and longitudinal study. Arthritis Rheum 52:3850–3859

Bouxsein ML, Palermo L, Yeung C, Black DM (2002) Digital X-ray radiogrammetry predicts hip, wrist and vertebral fracture risk in elderly women: a prospective analysis from the study of osteoporotic fractures. Osteoporos Int 13:358–365

Camp JD, Ochsner HC (1931) The osseous changes in hyperparathyroidism associated with parathyroid tumor: a roentgenologic study. Radiology 17:63

Campbell SE, Phillips CD, Dubovsky E, Cail WS, Omary RA (1995) The value of CT in determining potential instability of simple wedge-compression fractures of the lumbar spine. AJNR Am J Neuroradiol 16:1385–1392

Chappard C, Kolta S, Fechtenbaum J, Dougados M, Roux C (1998) Clinical evaluation of spine morphometric X-ray absorptiometry. Br J Rheumatol 37:496–501

Chew FS (1991) Radiologic manifestations in the musculoskeletal system of miscellaneous endocrine disorders. Radiol Clin North Am 29:135–147

Cortet B, Dubois P, Boutry N, Bourel P, Cotten A, Marchandise X (1999) Image analysis of the distal radius trabecular network using computed tomography. Osteoporos Int 9:410–419

Cosman F, Herrington B, Himmelstein S, Lindsay R (1991) Radiographic absorptiometry: a simple method for determination of bone mass. Osteoporosis Int 2:34–38

Crespo R, Revilla M, Usabiago J, Crespo E, Garcia-Arino J, Villa LF, Rico H (1998) Metacarpal radiogrammetry by computed radiography in postmenopausal women with Colles' fracture and vertebral crush fracture syndrome. Calcif Tissue Int 62:470–473

Cummings SR, Melton III LJ, Felsenberg D (1995) National Osteoporosis Foundation Working Group on Vertebral Fracture. Report: Assessing vertebral fractures. J Bone Miner Res 10:518–523

Davies KM, Recker RR, Heaney RP (1993) Revisable criteria for vertebral deformity. Osteoporosis Int 3:265–270

Delmas PD, Genant HK, Adams JE (2005) Vertebral fracture initiative. [cited 2007; Available from: http://www.iofbonehealth.org/vfi/index-flash.html

Dent RV, Milne MD, Roussak NJ, Steiner G (1953) Abdominal topography in relation to senile osteoporosis of the spine. Br Med J 2:1082–1084

Dequeker J (1976) Quantitative radiology: radiogrammetry of cortical bone. Br J Radiol 49:912–920

Deyo RA, McNiesh LM, Cone III RO (1985) Observer variability in the interpretation of lumbar spine radiographs. Arthritis Rheum 28:1066–1070

Diez A, Puig J, Serrano S, Marinoso M-L, Bosch J, Marrugat J (1994) Alcohol-induced bone disease in the absence of severe chronic liver damage. J Bone Miner Res 9:825–831

Doyle FH, Gutteridge DH, Joplin GF, Fraser R (1967) An assessment of radiological criteria used in the study of spinal osteoporosis. Brit J Radiol 40:241–250

Eastell R, Cedel SL, Wahner HW, Riggs BL, Melton LJ III (1991) Classification of vertebral fractures. J Bone Miner Res 6:207–215

Ekman A, Michaelsson K, Petren-Mallmin M, Ljunghall S, Mallmin H (2001) DXA of the hip and heel ultrasound but not densitometry of the fingers can discriminate female hip fracture patients from controls: a comparison between four different methods. Osteoporos Int 12:185–191

Evans RA, MdDonnell GD, Schieb M (1978) Metacarpal cortical area as an index of bone mass. Br J Radiol 51:428–431

Evans SF, Nicholson PHF, Haddaway MJ, Davie MWJ (1993) Vertebral morphometry in women aged 50–81 years. Bone Mineral 21:29–40

Falch JA, Sandvik L (1990) Perimenopausal appendicular bone loss: a 10-year prospective study. Bone 11:425–428

Ferrar L, Jiang G, Barrington NA, Eastell R (2000) Identification of vertebral deformities in women: comparison of radiological assessment and quantitative morphometry using morphometric radiography and morphometric X-ray absorptiometry. J Bone Miner Res 15:575–585

Ferrar L, Jiang G, Eastell R (2001) Short-term precision for morphometric X-ray absorptiometry. Osteoporos Int 12:710–715

Ferrar L, Jiang G, Adams J, Eastell R (2005) Identification of vertebral fractures: an update. Osteoporos Int 16:717–728

Fletcher H (1947) Anterior vertebral wedging – frequency and significance. AJR Am J Roentgenol 57:232–238

Froberg PK, Braunstein EM, Buckwalter KA (1996) Osteonecrosis, transient osteoporosis, and transient bone marrow edema: current concepts. Radiol Clin North Am 34:273–291

Frost HM (1964) Dynamics of bone remodelling. In: Frost HM (ed) Bone biodynamics. Little Brown, Boston, pp 315–334

Gallagher JC (1990) The pathogenesis of osteoporosis. Bone Miner 9:215–227

Garn SM, Rohmann CG, Wagner B (1967) Bone loss as a general phenomenon of man. Fed Proc 26:1729–1736

Garton MJ, Robertson EM, Gilbert FJ, Gomersall L, Reid DM (1994) Can radiologists detect osteopenia on plain radiographs? Clin Radiol 49:118–122

Gellman H, Keenan MA, Stone L, Hardy SE, Waters RL, Stewart C (1992) Reflex sympathetic dystrophy in brain-injured patients. Pain 51:307–311

Genant HK, Heck LL, Lanzl LH, Rossmann K, Vander Horst J, Paloyan E (1973) Primary hyperparathyroidism. A comprehensive study of clinical, biochemical and radiographic manifestations. Radiology 109:513–519

Genant HK, Vander Horst J, Lanzl LH, Mall JC, Doi K (1974) Skeletal demineralization in primary hyperparathyroidism. In: Mazess RB (ed) Proceedings of international conference on bone mineral measurement. National Institute of Arthritis, Metabolism and Digestive Diseases, Washington, DC, p 177

Genant HK, Doi K, Mall JC, Sickles EA (1977) Direct radiographic magnification for skeletal radiology. Radiology 123:47–55

Genant HK (1990) Radiographic assessment of the effects of intermittent cyclical treatment with etidronate. In:

Christiansen C, Overgaard K (eds) Third International Conference on Osteoporosis, Osteopress ApS, Copenhagen, p 2047–2054
Genant HK, Wu CY, van Kuijk C, Nevitt M (1993) Vertebral fracture assessment using a semi-quantitative technique. J Bone Miner Res 8:1137–1148
Genant HK, Jergas M, van Kuijk C (1995) Vertebral fracture in osteoporosis. Radiology Research and Education Foundation, San Francisco
Genant HK, Jergas M, Palermo L, Nevitt M, San Valentin R, Black D, Cummings SR (1996) Comparison of semiquantitative visual and quantitative morphometric assessment of prevalent and incident vertebral fractures in osteoporosis. J Bone Miner Res 11:984–996
Geraets W, Van der Stelt P, Lips P, Van Ginkel F (1998) The radiographic trabecular pattern of hips in patients with hip fractures and in elderly control subjects. Bone 22:165–173
Geusens P, Dequeker J, Verstraeten A, Nijs J (1986) Age-, sex-, and menopause-related changes of vertebral and peripheral bone: population study using dual and single photon absorptiometry and radiogrammetry. J Nucl Med 27:1540–1549
Gil HC, Levine SM, Zoga AC (2006) MRI findings in the subchondral bone marrow: a discussion of conditions including transient osteoporosis, transient bone marrow edema syndrome, SONK, and shifting bone marrow edema of the knee. Semin Musculoskelet Radiol 10:177–186
Goerres GW, Frey D, Hany TF, Seifert B, Hauselmann HJ, Studer A, Hauser D, Zilic N, Michel BA, Hans D, Uebelhart D (2007) Digital X-ray radiogrammetry better identifies osteoarthritis patients with a low bone mineral density than quantitative ultrasound. Eur Radiol 17:965–974
Grados F, Roux C, de Vernejoul MC, Utard G, Sebert JL, Fardellone P (2001) Comparison of four morphometric definitions and a semiquantitative consensus reading for assessing prevalent vertebral fractures. Osteoporos Int 12:716–722
Greenspan SL, Greenspan FS (1999) The effect of thyroid hormone on skeletal integrity. Ann Intern Med 130:750–758
Griffith GC, Nichols G, Ashey JD, Flannagan B (1965) Heparin osteoporosis. JAMA 193:85–88
Griffiths HJ, Virtama P (1990) Cortical thickness and trabecular pattern of the femoral neck as a measure of osteopenia. Invest Radiol 25:1116–1119
Guermazi A, Mohr A, Grigorian M, Taouli B, Genant HK (2002) Identification of vertebral fractures in osteoporosis. Semin Musculoskelet Radiol 6:241–252
Guerra JJ, Steinberg ME (1995) Distinguishing transient osteoporosis from avascular necrosis of the hip. J Bone Joint Surg 77:616–624
Hagiwara S, Yang S-O, Dhillon MS et al (1993) Precision and accuracy of photodensitometry of metacarpal bone (digital image processing). J Bone Miner Res 8[Suppl 1]:S 346
Hagiwara S, Engelke K, Takada M, Yang SO, Grampp S, Dhillon MS, Genant HK (1998) Accuracy and diagnostic sensitivity of radiographic absorptiometry of the second metacarpal. Calcif Tissue Int 62:95–98
Hanscom DA, Winter RB, Lutter L, Lonstein JE, Bloom BA, Bradford DS (1992) Osteogenesis imperfecta. Radiographic classification, natural history, and treatment of spinal deformities. J Bone Joint Surgery 74:598–616
Hansen M, Overgaard K, Nielsen V, Jensen G, Gotfredsen A, Christiansen C (1992) No secular increase in the prevalence of vertebral fractures due to postmenopausal osteoporosis. Osteoporosis Int 2:241–246
Hayashi Y, Yamamoto K, Fukunaga M, Ishibashi T, Takahashi K, Nishii Y (1990) Assessment of bone mass by image analysis of metacarpal bone roentgenograms: a quantitative digital image processing (DIP) method. Radiation medicine 8:173–178
Hayes CW, Conway WF (1991) Hyperparathyroidism. Radiol Clin North Am. 29:85–96
Hayes CW, Conway WF, Daniel WW (1993) MR imaging of bone marrow edema pattern: transient osteoporosis, transient bone marrow edema syndrome, or osteonecrosis. Radiographics 13:1001–1011
Hedlund LR, Gallagher JC (1988) Vertebral morphometry in diagnosis of spinal fractures. Bone Mineral 5:59–67
Heimann WG, Freiberger RH (1969) Avascular necrosis of the femoral and humeral heads after high-dosage corticosteroid therapy. N Engl J Med 263:672–674
Helela T, Virtama P (1970) Cortical thickness of long bones in different age groups. Symposium ossium. Livingstone, London, pp 238–240
Heuck F, Schmidt E (1960) Die quantitative Bestimmung des Mineralgehaltes des Knochens aus dem Röntgenbild. Fortschr Röntgenstr 93:523–554
Hodge HC, Bale WF, Warren SL, van Huysen G (1935) Factors influencing the quantitative measurement of the roentgen-ray absorption of tooth slabs. Am J Roentgenol 34:817–838
Hopper JL, Seeman E (1994) The bone density of twins discordant for tobacco use. N Engl J Med 330:387–392
Horsman A, Simpson M (1975) The measurement of sequential changes in cortical bone geometry. Br J Radiol 48:471–476
Hurel SJ, Kendall-Taylor P (1997) Avascular necrosis secondary to postoperative steroid therapy. Br J Neurosurg 11:356–358
Hurxthal L (1968) Measurement of anterior vertebral compressions and biconcave vertebrae. AJR Am J Roentgenol 103:635–644
Jacobs-Kosmin D, Sandorfi N, Murray H, Abruzzo JL (2005) Vertebral deformities identified by vertebral fracture assessment: associations with clinical characteristics and bone mineral density. J Clin Densitom 8:267–272
Jensen GF, McNair P, Boesen J, Hegedüs V (1984) Validity in diagnosing osteoporosis. Europ J Radiol 4:1–3
Jensen KK, Tougaard L (1981) A simple X-ray method for monitoring progress of osteoporosis. Lancet 2:19–20
Jergas M, San Valentin R (1995) Techniques for the assessment of vertebral dimensions in quantitative morphometry. In: Genant HK, Jergas M, van Kuijk C (eds) Vertebral fracture in osteoporosis. Radiology Research and Education Foundation, San Francisco, pp 163–88
Jergas M, Uffmann M, Escher H, Schaffstein J, Nitzschke E, Köster O (1994a) Visuelle Beurteilung konventioneller Röntgenaufnahmen und duale Röntgenabsorptiometrie in der Diagnostik der Osteoporose. Z Orthop Grenzgeb 132:91–98
Jergas M, Uffmann M, Escher H, Glüer CC, Young KC, Grampp S, Köster O, Genant HK (1994b) Interobserver variation in the detection of osteopenia by radiography and comparison with dual X-ray absorptiometry (DXA) of the lumbar spine. Skeletal Radiol 23:195–199

Jhamaria NL, Lal KB, Udawat M, Banerji P, Kabra SG (1983) The trabecular pattern of the calcaneum as an index of osteoporosis. J Bone Joint Surg 65-B:195–198

Jorgensen JT, Andersen PB, Rosholm A, Bjarnason NH (2000) Digital X-ray radiogrammetry: a new appendicular bone densitometric method with high precision. Clin Physiol 20:330–335

Kainberger F, Traindl O, Baldt M, Helbich T, Breitenseher M, Seidl G, Kovarik J (1992) Renale Osteodytrophie: Spektrum der Röntgensymptomatik bei modernen Formen der Nierentransplantation und Dauerdialysetherapie. Fortschr Röntgenstr 157:501–505

Kalidis L, Felsenberg D, Kalender W, Eidloth H, Wieland E (1992) Morphometric analysis of digitized radiographs: description of automatic evaluation. In: Ring EFG (ed) Current research in osteoporosis and bone mineral measurement II: 1992. British Institute of Radiology, Bath, pp 14–16

Kalla AA, Meyers OL, Parkyn ND, Kotze TJvW (1989) Osteoporosis screening – radiogrammetry revisited. Br J Rheumatol 28:511–517

Kalla AA, Kotze TJvW, Meyers OL (1992) Metacarpal bone mass in systemic lupus erythematotus. Clin Rheumatol 11:475–482

Kienböck R (1940) Osteomalazie, Osteoporose, Osteopsathyrose, porotische Kyphose. Fortschr Röntgenstr 61:159

Kiratli BJ (1996) Immobilization osteopenia. In: Marcus R, Feldman D, Kelsey J (eds) Osteoporosis. Academic Press, San Diego, pp 833–853

Kleerekoper M, Parfitt AM, Ellis BI (1984) Measurement of vertebral fracture rates in osteoporosis. In: Christiansen C, Arnaud CD, Nordin BEC, Parfitt AM, Peck WA, Riggs BL (eds) Copenhagen International Symposium on Osteoporosis June 3–8, 1984; Department of Clinical Chemistry, Glostrup Hospital, Copenhagen, p 103–108

Kleerekoper M, Nelson DA, Peterson EL, Tilley BC (1992) Outcome variables in osteoporosis trials. Bone 13:S29–S34

Kohlmeyer L, Gasner C, Marcus R (1993) Bone mineral status of women with Marfan syndrome. Am J Med 95:568–572

Koot VC, Kesselaer SM, Clevers GJ, de Hooge P, Weits T, van der Werken C (1996) Evaluation of the Singh index for measuring osteoporosis. J Bone Joint Surg Br 78:831–834

Kotowicz MA, Melton III LJ, Cooper C, Atkinson EJ, O'Fallon WM, Riggs LB (1994) Risk of hip fracture in women with vertebral fracture. J Bone Miner Res 9:599–605

Kriegshauser JS, Swee RG, McCarthy JT, Hauser MF (1987) Aluminum toxicity in patients undergoing dialysis: radiographic findings and prediction of bone biopsy results. Radiology 164:399–403

Krokowski E, Schlungbaum W (1959) Die Objektivierung der röntgenologischen Diagnose "Osteoporose". Fortschr Röntgenstr 91:740–746

Laan RF, Buijs WC, van Erning LJ, Lemmens JA, Corstens FH, Ruijs SH, van de Putte LB, van Riel PL (1993) Differential effects of glucocorticoids on cortical appendicular and cortical vertebral bone mineral content. Calcif Tissue Int 52:5–9

Lachmann E, Whelan M (1936) The roentgen diagnosis of osteoporosis and its limitations. Radiology 26:165–177

Laib A, Ruegsegger P (1999) Comparison of structure extraction methods for in vivo trabecular bone measurements. Comput Med Imaging Graph 23:69–74

Lecouvet F, Vande Berg B, Maldague B, Michaux L, Laterre E, Michaux J, Ferrant A, Malghem J (1997a) Vertebral compression fractures in multiple myeloma. Part I. Distribution and appearance at MR imaging. Radiology 204:195–199

Lecouvet F, Malghem J, Michaux L, Michaux J, Lehmann F, Maldague B, Jamart J, Ferrant A, Vande Berg B (1997b) Vertebral compression fractures in multiple myeloma. Part II. Assessment of fracture risk with MR imaging of spinal bone marrow. Radiology 204:201–205

LeGeros RZ (1994) Biological and synthetic apatites. In: Brown PW, Constantz B (eds) Hydroxyapatite and related materials. CRC Press, Boca Raton, pp 3–28

Leidig-Bruckner G, Genant HK, Minne HW, Storm T, Thamsborg G, Bruckner T, Sauer P, Schilling T, Soerensen OH, Ziegler R (1994) Comparison of a semiquantitative and a quantitative method for assessing vertebral fractures in osteoporosis. Osteoporosis Int 4:154–161

Leitha T, Staudenherz A, Korpan M, Fialka V (1996) Pattern recognition in five-phase bone scintigraphy: diagnostic patterns of reflex sympathetic dystrophy in adults. Eur J Nucl Med 23:256–262

Lenchik L, Rogers LF, Delmas PD, Genant HK (2004) Diagnosis of osteoporotic vertebral fractures: importance of recognition and description by radiologists. AJR Am J Roentgenol 183:949–958

Lespessailles E, Roux JP, Benhamou CL, Arlot ME, Eynard E, Harba R, Padonou C, Meunier P (1998) Fractal analysis of bone texture on os calcis radiographs compared with trabecular microarchitecture analyzed by histomorphometry. Calcif Tissue Int 63:121–125

Link T, Majumdar S, Konermann W, Meier N, Lin J, Newitt D, Ouyang X, Peters PE, Genant HK (1997) Texture analysis of direct magnification radiographs of vertebral specimens: correlation with bone mineral density and biomechanical properties. Acad Radiol 4:167–176

Link TM, Lin JC, Newitt D, Meier N, Waldt S, Majumdar S (1998) [Computer-assisted structure analysis of trabecular bone in the diagnosis of osteoporosis]. Der Radiologe 38:853–859

Mack PB, O'Brian AT, Smith JM, Bauman AW (1939) A method for estimating degree of mineralization of bones from tracings of roentgenograms. Science 89:467

Maggio D, Pacifici R, Cherubini A, Simonelli G, Luchetti M, Aisa MC, Cucinotta D, Adami S, Senin U (1997) Age-related cortical bone loss at the metacarpal. Calcif Tissue Int 60:94–97

Majumdar S, Kothari M, Augat P, Newitt DC, Link TM, Lin JC, Lang T, Lu Y, Genant HK (1998) High-resolution magnetic resonance imaging: three-dimensional trabecular bone architecture and biomechanical properties. Bone 22:445–454

Majumdar S, Link TM, Augat P, Lin JC, Newitt D, Lane NE, Genant HK (1999) Trabecular bone architecture in the distal radius using magnetic resonance imaging in subjects with fractures of the proximal femur. Magnetic Resonance Science Center and Osteoporosis and Arthritis Research Group. Osteoporos Int 10:231–239

Malich A, Boettcher J, Pfeil A, Sauner D, Heyne JP, Petrovitch A, Hansch A, Linss W, Kaiser WA (2004) The impact of technical conditions of X-ray imaging on reproducibility and precision of digital computer-assisted X-ray radiogrammetry (DXR). Skeletal Radiol 33:698–703

McAfee PC, Yuan HA, Fredrickson BE, Lubicky JP (1983) The value of computed tomography in thoracolumbar fractures. An analysis of one hundred consecutive cases and a new classification. J Bone Joint Surg [Am] 65:461–473

McCloskey EV, Spector TD, Eyres KS, Fern ED, O'Rourke N, Vasikaran S, Kanis JA (1993) The assessment of vertebral deformity: a method for use in population studies and clinical trials. Osteoporosis Int 3:138–147

Meema HE (1991) Improved vertebral fracture threshold in postmenopausal osteoporosis by radiographic measurements: its usefulness in selection for preventative therapy. J Bone Miner Res 6:9–14

Meema HE, Meema S (1969) Cortical bone mineral density versus cortical thickness in the diagnosis of osteoporosis: a roentgenologic densitometric study. J Am Geriat Soc 17:120–141

Meema HE, Meema S (1972) Microradioscopic and morphometric findings in the hand bones with densitometric findings in the proximal radius in thyrotoxicosis and in renal osteodystrophy. Investigative Radiol 7:88

Meema S, Meema HE (1976) Menopausal bone loss and estrogen replacement. Isr J Med Sci 12:601–606

Meema HE, Meema S (1981) Radiogrammetry. In: Cohn SH (ed) Non-invasive measurements of bone mass. CRC Press, Boca Raton, pp 5–50

Meema HE, Meema S (1987) Postmenopausal osteoporosis: simple screening method for diagnosis before structural failure. Radiology 164:405–410

Meema HE, Meindok H (1992) Advantages of peripheral radiogrametry over dual-photon absorptiometry of the spine in the assessment of prevalence of osteoporotic vertebral fractures in women. J Bone Miner Res 7:897–903

Melton III LJ, Kan SH, Frye MA, Wahner HW, O'Fallon WM, Riggs BL (1989) Epidemiology of vertebral fractures in women. Am J Epidemiol 129:1000–1011

Meunier PJ, Bressot C, Vignon E et al (1978) Radiological and histological evolution of post-menopausal osteoporosis treated with sodium fluoride-vitamin D-calcium. Preliminary results. In: Courvoisier B, Donath A, Baud CA (eds) Fluoride and bone. Hans Huber Publishers, Bern, 263–276

Millard J, Augat P, Link TM, Kothari M, Newitt DC, Genant HK, Majumdar S (1998) Power spectral analysis of vertebral trabecular bone structure from radiographs: orientation dependence and correlation with bone mineral density and mechanical properties. Calcif Tissue Int 63:482–489

Minch CM, Kruse RW (1998) Osteogenesis imperfecta: a review of basic science and diagnosis. Orthopedics 21:558–567

Minne HW, Leidig G, Wüster C, Siromachkostov L, Baldauf G, Bickel R, Sauer P, Lojen M, Ziegler R (1988) A newly developed spine deformity index (SDI) to quantitate vertebral crush fractures in patients with osteoporosis. Bone Mineral 3:335–349

Molpus WM, Pritchard RS, Walker CW, Fitzrandolph RL (1991) The radiographic spectrum of renal osteodystrophy. Am Fam Physician 43:151–158

Mosekilde L, Eriksen EF, Charles P (1990) Effects of thyroid hormones on bone and mineral metabolism. Endocrinol Metab Clin North Am 19:35–63

Moulopoulos LA, Dimopoulos MA (1997) Magnetic resonance imaging of the bone marrow in hematologic malignancies. Blood 90:2127–2147

Murphey MD, Sartoris DJ, Quale JL, Pathria MN, Martin NL (1993) Musculoskeletal manifestations of chronic renal insufficiency. Radiographics 13:357–379

Mussolino ME, Looker AC, Madans JH, Edelstein D, Walker RE, Lydick E, Epstein RS, Yates AJ (1997) Phalangeal bone density and hip fracture risk. Arch Intern Med 157:433–438

Mussolino ME, Looker AC, Madans JH, Langlois JA, Orwoll ES (1998) Risk factors for hip fracture in white men: the NHANES I epidemiologic follow-up study. J Bone Miner Res 13:918–924

National Osteoporosis Foundation (NOF) (2000) Physician's guide to prevention and treatment of osteoporosis. Washington DC

Nelson D, Peterson E, Tilley B, O'Fallon W, Chao E, Riggs BL, Kleerekoper M (1990) Measurement of vertebral area on spine X-rays in osteoporosis: reliability of digitizing techniques. J Bone Miner Res 5:707–716

Nelson-Piercy C (1998) Heparin-induced osteoporosis. Scand J Rheumatol Suppl 107:68–71

Nielsen VAH, Pødenphant J, Martens S, Gotfredsen A, Riis BJ (1991) Precision in assessment of osteoporosis from spine radiographs. Europ J Radiol 13:11–14

Nordin BEC, Barnett E, MacGregor J, Nisbet J (1962) Lumbar spine densitometry. Br Med J I:1793–1796

Norman ME (1996) Juvenile osteoporosis. In: Favus MJ (ed) Primer on the metabolic diseases and disorders of mineral metabolism, 3rd edn. Lippincott-Raven, Philadelphia, pp 275–278

Nuzzo V, Lupoli G, Esposito Del Puente A, Rampone E, Carpinelli A, Del Puente AE, Oriente P (1998) Bone mineral density in premenopausal women receiving levothyroxine suppressive therapy. Gynecol Endocrinol 12:333–337

Olmez N, Kaya T, Gunaydin R, Vidinli BD, Erdogan N, Memis A (2005) Intra- and interobserver variability of Kleerekoper's method in vertebral fracture assessment. Clin Rheumatol 24:215–218

Oyen WJ, Arntz IE, Claessens RM, Van der Meer JW, Corstens FH, Goris RJ (1993) Reflex sympathetic dystrophy of the hand: an excessive inflammatory response? Pain 55:151–157

Palit G, Kerremans M, Gorissen J, Jacquemyn Y (2006) Transient bone marrow oedema of the femoral head in pregnancy – case report. Clin Exp Obstet Gynecol 33:244–245

Peacock M, Turner CH, Liu G, Manatunga AK, Timmerman L, Johnston CC Jr (1995) Better discrimination of hip fracture using bone density, geometry and architecture. Osteoporos Int 5:167–173

Pitt MJ (1991) Rickets and osteomalacia are still around. Radiol Clin North Am 29:97–118

Pitt MJ (1995) Rickets and osteomalacia. In: Resnick D (ed) Diagnosis of bone and joint disorders, 3rd edn. W.B. Saunders Company, Philadelphia, pp 1885–1922

Plato CC, Purifoy FE (1982) Age, sex and bilateral variability in cortical bone loss and measurements of the second metacarpal. Growth 46:100–112

Rea JA, Chen MB, Li J, Blake GM, Steiger P, Genant HK, Fogelman I (2000) Morphometric X-ray absorptiometry and morphometric radiography of the spine: a comparison of prevalent vertebral deformity identification. J Bone Miner Res 15:564–574

Reginato AJ, Falasca GF, Pappu R, McKnight B, Agha A (1999) Musculoskeletal manifestations of osteomalacia: report of 26 cases and literature review. Semin Arthritis Rheum 28:287–304

Resnick D (1981) The "rugger jersey" vertebral body. Arthritis Rheum 24:1191–1194

Resnick D (1995a) Hemoglobinopathies and other anemias. In: Resnick D (ed) Diagnosis of bone and joint disorders, 3rd edn. WB Saunders Company, Philadelphia, pp 2107–2146

Resnick D (1995b) Plasma cell dyscrasias and dysgammaglobulinemias. In: Resnick D (ed) Diagnosis of bone and joint disorders, 3rd edn. WB Saunders Company, Philadelphia, pp 2147–2189

Resnick D, Niwayama G (1995a) Parathyroid disorders and renal osteodystrophy. In: Resnick D (ed) Diagnosis of bone and joint disorders, 3rd edn. WB Saunders, Philadelphia, pp 2012–2075

Resnick D, Niwayama G (1995b) Osteoporosis. In: Resnick D (ed) Diagnosis of bone and joint disorders, 3rd edn. WB Saunders Company, Philadelphia, pp 1783–1853

Richardson ML, Pozzi-Mucelli RS, Kanter AS, Kolb FO, Ettinger B, Genant HK (1986) Bone mineral changes in primary hyperparathyroidism. Skeletal Radiol 15:85–95

Rico H, Hernandez ER (1989) Bone radiogrametry: caliper versus magnifying glass. Calcif Tissue Int 45:285–287

Riggs BL, Melton LJ (1983) Evidence for two distinct syndromes of involutional osteoporosis. Am J Med 75:899–901

Rosenberg AE (1991) The pathology of metabolic bone disease. Radiol Clin North Am 29:19–35

Rosenthal DI, Gregg GA, Slovik DM, Neer RM (1987) A comparison of quantitative computed tomography to four techniques of upper extremity bone mass measurement. In: Genant HK (ed) Osteoporosis Update 1987. Radiology Research and Education Foundation, San Francisco, pp 87–93

Ross PD, Davis JW, Epstein RS, Wasnich RD (1991) Pre-existing fractures and bone mass predict vertebral fracture incidence in women. Ann Intern Med 114:919–923

Ross PD, Genant HK, Davis JW, Miller PD, Wasnich RD (1993a) Predicting vertebral fracture incidence from prevalent fractures and bone density among non-black, osteoporotic women. Osteoporosis Int 3:120–126

Ross PD, Yhee YK, He Y-F, Davis JW, Kamimoto C, Epstein RS, Wasnich RD (1993b) A new method for vertebral fracture diagnosis. J Bone Miner Res 8:167–174

Ross PD, Huang C, Davis JW, Imose K, Yates J, Vogel J, Wasnich RD (1995) Predicting vertebral deformity using bone densitometry at various skeletal sites and calcaneus ultrasound. Bone 16:325–332

Rupp WM, McCarthy HB, Rohde TD, Blackshear PJ, Goldenberg FJ, Buchwald H (1982) Risk of osteoporosis in patients treated with long-term intravenous heparin therapy. Curr Surg 39:419–422

Sackler JP, Liu L (1973) Heparin-induced osteoporosis. Br J Radiol 46:548–550

Saito JK, Davis JW, Wasnich RD, Ross PD (1995) Users of low-dose glucocorticoids have increased bone loss rates: a longitudinal study. Calcif Tissue Int 57:115–119

Sarangi PP, Ward AJ, Smith EJ, Staddon GE, Atkins RM (1993) Algodystrophy and osteoporosis after tibial fractures. J Bone Joint Surg Br 75:450–452

Sauer P, Leidig G, Minne HW, Duckeck G, Schwarz W, Siromachkostov L, Ziegler R (1991) Spine deformity index (SDI) versus other objective procedures of vertebral fracture identification in patients with osteoporosis. J Bone Miner Res 6:227–238

Saville PD (1967) A quantitative approach to simple radiographic diagnosis of osteoporosis: its application to the osteoporosis of rheumatoid arthritis. Arthritis Rheumatism 10:416–422

Schwartz EN, Steinberg D (2005) Detection of vertebral fractures. Curr Osteoporos Rep 3:126–135

Schwartzman RJ, McLellan TL (1987) Reflex sympathetic dystrophy: a review. Arch Neurol 44:555–561

Seeman E, Szmukler GI, Formica C, Tsalamandris C, Mestrovic R (1992) Osteoporosis in anorexia nervosa: the influence of peak bone density, bone loss, oral contraceptive use, and exercise. J Bone Miner Res 7:1467–1474

Shaughnessy SG, Hirsh J, Bhandari M, Muir JM, Young E, Weitz JI (1999) A histomorphometric evaluation of heparin-induced bone loss after discontinuation of heparin treatment in rats. Blood 93:1231–1236

Singh YM, Nagrath AR, Maini PS (1970) Changes in trabecular pattern of the upper end of the femur as an index of osteoporosis. J Bone Joint Surg 52-A:457–467

Singh YM, Riggs BL, Beabout JW, Jowsey J (1972) Femoral trabecular-pattern index for evaluation of spinal osteoporosis. Ann Int Med 77:63–67

Smith R (1995) Idiopathic juvenile osteoporosis: experience of twenty-one patients. Br J Rheumatol 34:68–77

Smith RW, Eyler WR, Mellinger RC (1960) On the incidence of senile osteoporosis. Ann Int Med 52:773–781

Smith R, Stevenson JC, Winearls CG, Woods CG, Wordsworth BP (1985) Osteoporosis of pregnancy. Lancet 1:1178–1180

Smith-Bindman R, Cummings SR, Steiger P, Genant HK (1991) A comparison of morphometric definitions of vertebral fracture. J Bone Miner Res 6:25–34

Solomon BL, Wartofsky L, Burman KD (1993) Prevalence of fractures in postmenopausal women with thyroid disease. Thyroid 3:17–23

Spencer NE, Steiger P, Cummings SR, Genant HK (1990) Placement for points for digitizing spine films. J Bone Miner Res 5[Suppl 2]:S247

Stäbler A, Baur A, Bartl R, Munker R, Lamerz R, Reiser MF (1996) Contrast enhancement and quantitative signal analysis in MR imaging of multiple myeloma: assessment of focal and diffuse growth patterns in marrow correlated with biopsies and survival rates. AJR Am J Roentgenol 167:1029–1036

Steiger P, Weiss H, Stein JA (1993) Morphometric X-ray absorptiometry of the spine: a new method to assess vertebral osteoporosis. In: Christiansen C, Riis B (eds) Proceedings of the 4th International Symposium on Osteoporosis and Consensus Development Conference, 1993, Hong Kong, p 292

Steiger P, Cummings SR, Genant HK, Weiss H (1994) Morphometric X-ray absorptiometry of the spine: correlation in vivo with morphometric radiography. Osteoporosis Int 4:238–244

Stein I (1937) The evaluation of bone density in the roentgenogram by the use of an ivory wedge. AJR Am J Roentgenol 37:678–682

Steinbach HL, Kolb FO, Gilfillan R (1954) A mechanism of the production of pseudofractures in osteomalacia (Milkman's syndrome). Radiology 62:388

Steinbach HL, Gordan GS, Eisenberg E, Carne JT, Silverman S, Goldman L (1961) Primary hyperparathyroidism: a correlation of roentgen, clinical, and pathologic features. Am J Roentgenol Radium Ther Nucl Med 86:239–243

Steven GD (1947) "Standard bone". A description of radiographic technique. Ann Rheum Dis 6:184–185

Sudeck P (1901) Über die akute (reflectorische) Knochenatrophie nach Entzündungen und Verletzungen an den Extremitäten und ihre klinischen Erscheinungen. RöFo 5:277

Sundaram M (1989) Renal osteodystrophy. Skeletal Radiol 18:415–426

Takada M, Engelke K, Hagiwara S, Grampp S, Jergas M, Glüer CC, Genant HK (1997) Assessment of osteoporosis: comparison of radiographic absorptiometry of the phalanges and dual X-ray absorptiometry of the radius and the lumbar spine. Radiology 202:759–763

Tehranzadeh J, Tao C (2004) Advances in MR imaging of vertebral collapse. Semin Ultrasound CT MR 25:440–460

Todorovic Tirnanic M, Obradovic V, Han R, Goldner B, Stankovic D, Sekulic D, Lazic T, Djordjevic B (1995) Diagnostic approach to reflex sympathetic dystrophy after fracture: radiography or bone scintigraphy? Eur J Nucl Med 22:1187–1193

Toh SH, Claunch BC, Brown PH (1985) Effect of hyperthyroidism and its treatment on bone mineral content. Arch Intern Med 145:883–886

Toledo VA, Jergas M (2006) Age-related changes in cortical bone mass: data from a German female cohort. Eur Radiol 16:811–817

Trepman E, King TV (1992) Transient osteoporosis of the hip misdiagnosed as osteonecrosis on magnetic resonance imaging. Orthop Rev 21:1089–1091, 1094–1098

Trouerbach WT, Birkenhäger JC, Collette BJA, Drogendijk AC, Schmitz PIM, Zwamborn AW (1987) A study on the phalanx bone mineral content in 273 normal pre- and post-menopausal females (transverse study of age-dependent bone loss). Bone Miner 3:53–62

Trouerbach WT, Vecht-Hart CM, Collette HJA, Slooter GD, Zwamborn AW, Schmitz PIM (1993) Cross-sectional and longitudinal study of age-related phalangeal bone loss in adult females. J Bone Miner Res 8:685–691

Urist MR (1960) Observations bearing on the problem of osteoporosis. In: Rodahl K, Nicholson JT, Brown EM Jr (eds) Bone as a tissue. McGraw-Hill, New York, pp 18–45

van Rijn RR, Grootfaam DS, Lequin MH, Boot AM, van Beek RD, Hop WC, van Kuijk C (2004) Digital radiogrammetry of the hand in a pediatric and adolescent Dutch Caucasian population: normative data and measurements in children with inflammatory bowel disease and juvenile chronic arthritis. Calcif Tissue Int 74:342–350

van Rijn RR, Boot A, Wittenberg R, van der Sluis IM, van den Heuvel-Eibrink MM, Lequin MH, de MuinckKeizer-Schrama SM, Van Kuijk C (2006) Direct X-ray radiogrammetry versus dual-energy X-ray absorptiometry: assessment of bone density in children treated for acute lymphoblastic leukaemia and growth hormone deficiency. Pediatr Radiol 36:227–232

Versluis RGJA, Petri H, Vismans FJFE, van de Ven CM, Springer MP, Papapoulos SE (2000) The relationship between phalangeal bone density and vertebral deformities. Calcif Tissue Int 66:1–4

Virtama P (1960) Uneven distribution of bone mineral and covering effect of non-mineralized tissue as reasons for impaired detectability of bone density from roentgenograms. Ann Med Int Fenn 49:57–65

Walenga JM, Bick RL (1998) Heparin-induced thrombocytopenia, paradoxical thromboembolism, and other side-effects of heparin therapy. Med Clin North Am 82:635–658

Wu CY, Li J, Jergas M, Genant HK (1995) Comparison of semiquantitative and quantitative techniques for the assessment of prevalent and incident vertebral fractures. Osteoporosis Int 5:354–370

Wu C, van Kuijk C, Li J, Jiang Y, Chan M, Countryman P, Genant HK (2000) Comparison of digitized images with original radiography for semiquantitative assessment of osteoporotic fractures. Osteoporos Int 11:25–30

Zionts LE, Nash JP, Rude R, Ross T, Stott NS (1995) Bone mineral density in children with mild osteogenesis imperfecta. J Bone Joint Surg Br 77:143–147